공학박사학위논문

Modeling and Mapping of Combined Noise Annoyance for Aircraft and Road Traffic Noise

항공기와 도로 교통 소음의 복합 소음에 대한 불쾌감 평가 모델 개발 및 인지적 소음지도 작성

2019년 8월

서울대학교 대학원

기계항공공학부

전 찬 일

항공기와 도로 교통 소음의 복합 소음에 대한 불쾌감 평가 모델 개발 및 인지적 소음지도 작성

Modeling and mapping of combined noise annoyance for aircraft and road traffic noise

지도교수 이 수 갑

이 논문을 공학박사 학위논문으로 제출함

2019 년 4 월

서울대학교 대학원

기계항공공학부

전 찬 일

전찬일의 공학박사 학위논문을 인준함

2019 년 6 월

위 원 장 : 李管中

부위원장 : 李秀甲

위　　원 : 鄭完燮

위　　원 : 林昌雨

위　　원 : 洪枝英

Abstract

Modeling and Mapping of Combined Noise Annoyance for Aircraft and Road Traffic Noises

Chanil Chun

Department of Mechanical and Aerospace Engineering

Graduate School

Seoul National University

Since the transportation system became complex, exposure to combined aircraft and road traffic noises is common in these days. As the reaction to the combined noises is different from single noises, it should be evaluated for the annoyance from combined aircraft and road traffic noises. Previous studies have assessed the annoyance factor with physical noise levels. However, annoyance is a psychoacoustical factor so that it must be evaluated within the same category. By many researches, loudness is proved to have high relationship with noise annoyance so that in this research, annoyance models of combined aircraft and road traffic noises are studied with the loudness factor.

Before developing annoyance models, a partial loudness model for combined noises incorporating with binaural inhibition is proposed and validated. As the new model well predicts the partial loudness from the combined noises, it is applied for the calculation of annoyance from complex noises.

The short-term annoyance model is developed through the jury tests. By the evaluation of the annoyance for combined aircraft and road traffic noises from test subjects and logistic regression of partial loudness with test results, a short-term loudness model of combined noise is derived.

The long-term loudness model is deduced from the survey data and noise maps. From the noise maps of aircraft and road traffic noises, noise levels at the survey regions are known, and they are converted to the partial loudness values with partial loudness model with binaural inhibition. Logistic regression of the partial loudness with annoyance data from field survey produced the long-term annoyance model for combined noises of aircraft and road traffic noise and it is implanted to noise mapping program to depict the annoyance map. Annoyance maps of aircraft and road traffic noise presents how annoyed the residents are and also show the background noise effect as the former noise maps could not.

Keywords: Combined noises, Partial Loudness, Annoyance model, Annoyance map

Student Number: 2013-20711

Contents

List of Tables

List of Figures

Chapter. 1

Introduction

1.1 Background

These days, transportation systems complexify so that population of noise exposure from multiple noise sources are increasing. For example, residents who live near the airport are also exposed by road traffic noise as the road traffic system developed, and inhabitants who live vicinity of railways are prone to suffer from road traffic noise due to increment of roads near railway stations. The degree of noise exposure became severe so that exposed people are annoyed by noise sources. These being so, many countries already settled the regulations of noise levels and sources [1,2].

However, despite these restrictions, exposures from multiple noise sources are not yet considered, rather combined noises are treated as the sum of single noise sources or they are regulated for each noise source [3].

Many researches have been studied about combined noise exposure and their effects on health [4,5,6]. It is revealed that noise exposure causes hearing loss as an auditory health effect and sleep disturbance, hypertension and cardiovascular diseases as non-auditory effects.

The most epidemic effect of noise is perceived annoyance. It is the main issue of noise exposure from many other countries [7,8,9].

Earlier researchers attempted to quantify the perceived annoyance from noise exposure and suggested models that calculate annoyance from physical factors of noise, such as $\mathbf{L}_{eq}$ or $\mathbf{L}_{dn}$ [10].

Nevertheless, these models only consider the intensity factor of noise so that they omit the frequency characteristics. This means that same level of two different noise are calculated to same annoyance degree without regard to their spectrums or source types. Many studies have shown that their results are differ from real situations [11,12]. To overcome this shortcoming, recent study proposes a new model to quantify the annoyance of noise by containing not only acoustical factors but also non-acoustical values [13,14]. Yet it lacks applicability as it is more complicated model than earlier ones. Also, earlier models treated the annoyance of combined noises as a sum of annoyance from each noise source, ignoring the contribution of each source on total annoyance factor [11].

Additionally, binaural effect is not considered in former methods. Although many studies have been conducted to reveal the effect of binaural hearing [15], none of former models adopted it for the deduction of annoyance on single noise sources as well as combined noises. Some methods treated the binaural effect as the twice of single channel results, yet it shows different from laboratory test results [16].

From all the reasons above, an improved models of combined noise annoyance from aircraft and road traffic noise regarding binaural effect are suggested in this research. These models include intensity factors as well as frequency characteristics and are simple as former models so that applicability is high. In addition, binaural effect, especially binaural inhibition is applied to calculate the annoyance of combined noises. Finally, the newly suggested models consider the contribution of each noise source on annoyance so that different noise levels with different source types are considered individually for evaluating combined annoyance.

1.2 Literature Reviews

1.2.1Annoyance Models from Combined Noises

Many researches have attempted to quantify the annoyance of combined noises from transportation noises. In this section, the models that calculate the annoyance from combined noises are introduced regarding developing methods.

1.2.1.1 Classical Models

The strongest component model is the method to derive total annoyance from the maximum of specific annoyance by the combined noise sources and it is expressed as equation 1.1.

$$A_T = \max(A_1, A_2) \tag{1.1}$$

A_T is the total annoyance and A_1, A_2 are the specific annoyance from each of the combined noise sources. Although many studies revealed that it has good predictions with great distinctions between two specific annoyances [17,18,19], poor reliability occurs for the similar or same specific annoyances [8,20].

The linear regression model calculates the total annoyance by a summation of weighted specific annoyance and is expressed as equation 1.2 [21].

$$A_T = a_1 A_1 + a_2 A_2 + b \tag{1.2}$$

This model gives an idea to many researchers how to treat each annoyance component for derivation of total annoyance but has lower predictability than the strongest component model [18].

The vector summation model adopted the method from vector summation and is shown in equation 1.3 [17].

$$A_T = a\left({A_1}^2 + {A_2}^2 + 2A_1A_2\cos\alpha_{12}\right)^{1/2} + b \tag{1.3}$$

This model overpredicts the total annoyance and $\boldsymbol{\alpha_{12}}$ is a new factor that must be determined for every new calculation of combined noises [18].

The energy summation model derives the total annoyance from the total noise level, $\boldsymbol{L_T}$ and is expressed as equation 1.4.

$$\boldsymbol{A_T = aL_T + b} \tag{1.4}$$

This model has inaccuracy in the case of same total noise level with different source contributions [22].

The independent effects model deduces the total annoyance from each noise level of combined noise components which is shown as equation 1.5.

$$\boldsymbol{A_T = a_1L_1 + a_2L_2 + b} \tag{1.5}$$

This model is developed from the energy summation model yet to explain the relationship between the psychoacoustic factor, annoyance, and the physical factor [11].

The energy difference model obtains the total annoyance from the total noise level and the difference between the noise levels of two noise sources and is presented as equation 1.6.

$$\boldsymbol{A_T = aL_T + b|L_1 - L_2| + c} \tag{1.6}$$

This model also needs an extra explanation for the relationship between total annoyance factor and the physical noise factor [11].

All the above models derive total annoyance from either noise levels or the annoyance factor. However, low accuracy and lack of relationship between physical factor and psychoacoustical value appear to evoke the necessities to be proved. From these reasons, dose-response model is developed which is introduced in section 1.1.1.2.

1.2.1.2 Dose-Response Model

The first dose-response model for the combined noise annoyance is suggested by Miedema [22]. It is the method of deriving annoyance from the field survey data. The model is derived by the method from Vos called annoyance equivalent model [23]. The annoyance equivalents model deduces the total annoyance from the equivalent annoyance value that evoked by each noise source. Translation of annoyance from one noise source to the equivalent noise levels and calculation of annoyance that derives from the sum of the two noise levels is the main procedure. Miedema suggested the model with two noise indices which are *DNL* and *DENL*. Those factors are the noise levels that weigh the level of evening and night exposure. *DNL* and *DENL* are expressed as equation 1.7 and 1.8.

$$\boldsymbol{DNL = 10log[(\frac{15}{24}) \times 10^{\frac{LD}{10}} + (\frac{9}{24}) \times 10^{\frac{LN+10}{10}}]} \qquad (1.7)$$

$$\boldsymbol{DENL = 10log[(\frac{12}{24}) \times 10^{\frac{LD}{10}} + (\frac{4}{24}) \times 10^{\frac{LE+5}{10}} + (\frac{8}{24}) \times 10^{\frac{LN+10}{10}}]} \tag{1.8}$$

$\boldsymbol{LD}$, $\boldsymbol{LE}$ and $\boldsymbol{LN}$ are the A-weighted $\boldsymbol{L_{A_{eq}}}$ for day in 7-19h, evening in 19-23h, and night in 23-7h.

The procedures for deriving total annoyance from dose-response model are as follow.

(1) Derive the level of transportation noises, for example, aircraft, road traffic and railway($\boldsymbol{L_{air}}$, $\boldsymbol{L_{road}}$, and $\boldsymbol{L_{rail}}$)

(2) Calculate the annoyance from the aircraft and railway noise.

$$\boldsymbol{A_{air} = 2.16L_{air} - 89.7} \tag{1.9}$$

$$\boldsymbol{A_{rail} = 2.06L_{rail} - 107.5} \tag{1.10}$$

(3) Deduce the road traffic levels as reference of equally annoying levels from aircraft and railway noise.

$$\boldsymbol{L'_{air} = (A_{air} + 105.7)/2.21} \tag{1.11}$$

$$\boldsymbol{L'_{rail} = (A_{rail} + 105.7)/2.21} \tag{1.12}$$

(4) Calculate the total noise level from combined noises.

$$\boldsymbol{L = 10\log(10^{0.1\times L'_{air}} + 10^{0.1\times L_{road}} + 10^{0.1\times L'_{rail}})} \tag{1.13}$$

(5) Deduce the percentage of little annoyed, annoyed and highly annoyed for the combined noises.

$$\%\boldsymbol{LA} = -\mathbf{6.188} \times \mathbf{10^{-4}}(\boldsymbol{L} - \mathbf{32})^{\mathbf{3}} + \mathbf{5.379} \times \mathbf{10^{-2}}(\boldsymbol{L} - \mathbf{32})^{\mathbf{2}} + \mathbf{0.723}(\boldsymbol{L} - \mathbf{32}) \tag{1.14}$$

$$\%\boldsymbol{A} = \mathbf{1.732} \times \mathbf{10^{-4}}(\boldsymbol{L} - \mathbf{37})^{\mathbf{3}} + \mathbf{2.079} \times \mathbf{10^{-2}}(\boldsymbol{L} - \mathbf{37})^{\mathbf{2}} + \mathbf{0.566}(\boldsymbol{L} - \mathbf{37}) \tag{1.15}$$

$$\%\boldsymbol{HA} = \mathbf{9.994} \times \mathbf{10^{-4}}(\boldsymbol{L} - \mathbf{42})^{\mathbf{3}} - \mathbf{1.523} \times \mathbf{10^{-2}}(\boldsymbol{L} - \mathbf{42})^{\mathbf{2}} + \mathbf{0.538}(\boldsymbol{L} - \mathbf{42}) \tag{1.16}$$

For the case of *DENL*, same procedures with different annoyance values and percentage of annoyed are applied.

(1) Derive the level of transportation noises, for example, aircraft, road traffic and railway($\boldsymbol{L_{air}}$, $\boldsymbol{L_{road}}$, and $\boldsymbol{L_{rail}}$)

(2) Calculate the annoyance from the aircraft and railway noise.

$$\boldsymbol{A_{air}} = \mathbf{2.17}\boldsymbol{L_{air}} - \mathbf{91.4} \tag{1.17}$$

$$\boldsymbol{A_{rail}} = \mathbf{2.10}\boldsymbol{L_{rail}} - \mathbf{110.1} \tag{1.18}$$

(3) Deduce the road traffic levels as reference of equally annoying levels from aircraft and railway noise.

$$\boldsymbol{L'_{air}} = (\boldsymbol{A_{air}} + \mathbf{107.0})/\mathbf{2.22} \tag{1.19}$$

$$\boldsymbol{L'_{rail}} = (\boldsymbol{A_{rail}} + \mathbf{107.0})/\mathbf{2.22} \tag{1.20}$$

(4) Calculate the total noise level from combined noises.

$$\boldsymbol{L = 10\log(10^{0.1\times L'_{air}} + 10^{0.1\times L_{road}} + 10^{0.1\times L'_{rail}})} \tag{1.21}$$

(5) Deduce the percentage of little annoyed, annoyed, highly annoyed and expected annoyance for the combined noises.

$$\boldsymbol{\%LA = -6.235 \times 10^{-4}(L-32)^3 + 5.509 \times 10^{-2}(L-32)^2 + 0.6693(L-32)} \tag{1.22}$$

$$\boldsymbol{\%A = 1.795 \times 10^{-4}(L-37)^3 + 2.110 \times 10^{-2}(L-37)^2 + 0.5353(L-37)} \tag{1.23}$$

$$\boldsymbol{\%HA = 9.868 \times 10^{-4}(L-42)^3 - 1.436 \times 10^{-2}(L-42)^2 + 0.5118(L-42)} \tag{1.24}$$

$$\boldsymbol{EA = -9.154 \times 10^{-5}(L-32)^3 + 2.307 \times 10^{-2}(L-32)^2 + 0.537(L-32)} \tag{1.25}$$

The derived annoyance models from Miedema are widely used for the calculation of annoyance from combined transportation noises.

Although Miedema's models applied annoyance equivalent factor from the reference source, it still derives the psychoacoustic value, annoyance, from physical factor, the noise level, and it lacks the spectrum characteristics from each source. In addition, the applicability is limited only for the aircraft, road traffic and railway noises.

1.2.2 Psychoacoustical factors

In the evaluation of sound, physical factors, especially sound intensity, are deficient to express how people are affected by the target noise. For example, same noise level with different sources show distinct reaction to the sound. To overcome this phenomenon, many researches have been conducted to assess the sound incorporating psychophysical factors and from these efforts, psychoacoustics is developed [24].

In psychoacoustics, sound quality factors are defined with regarding to physical factors. Loudness is the factor related to sound intensity, sharpness and roughness are the values from frequency characteristics, and fluctuation strength is the factor regarding modulation frequencies. In this section, each factor of sound quality is described and annoyance model which covers all the psychoacoustic factors is shown.

1.2.2.1 Loudness

Loudness is a sensation regarding category of intensity. For the comparison of loudness magnitude, loudness level is introduced by Barkhausen. It is defined as the sound pressure level of 1-kHz tone in a plane wave and frontal incident that is as loud as the sound. The unit of the loudness level is “phon”. For example, a test sound which is as loud as 40 dB of 1-kHz tone has the loudness level of 40 phon. By the application of loudness level, equal-loudness contours are developed to visualize the loudness levels of given sounds. The unit of "sone" is also developed that 1 sone of sound is equally loud as 40 dB of 1-kHz tone noise.

To functionalize the calculation of loudness level, loudness models are developed and are introduced in section 1.2.3.

1.2.2.2 Sharpness

Sharpness is a sensation which is influenced by the spectral content and the center frequency of narrow-band noises. The unit of sharpness is "acum" which is the expression of sharp in Latin. As same method for loudness, sharpness is compared with the reference of 60 dB of 1-kHz tone. 1 acum is a narrow-band noise with one critical-band wide at a center frequency of 1-kHz regarding 60dB.

For the calculation of sharpness, a model of sharpness is suggested and is expressed as equation 1.26.

$$\boldsymbol{S = 0.11 \frac{\int_0^{24\ Bark} N' g(z) z dz}{\int_0^{24\ Bark} N' dz}}\ \mathbf{acum} \tag{1.26}$$

In the equation, $\boldsymbol{S}$ is the sharpness, denominator is the total loudness and numerator includes weighting factor $\boldsymbol{g}$ which is frequency dependent.

1.2.2.3 Fluctuation Strength

For the sound of modulated sounds, fluctuation strength and roughness occur. Fluctuation strength of modulated signal is generated with a modulation frequency about 20Hz, whether high modulation frequency gives the sensation of roughness. Roughness is described in section 1.2.2.4. The reference of fluctuation strength is 60dB, 1-kHz tone 100% amplitude modulated at 4Hz which produces 1 “vacil”. Experiments were conducted to formulate the fluctuation strength and the equation is shown as equation 1.27.

$$\boldsymbol{F_{BBN}} = \frac{\mathbf{5.8(1.25}\boldsymbol{m}\mathbf{-0.25)[0.05}\left(\frac{\boldsymbol{L_{BBN}}}{\boldsymbol{dB}}\right)\mathbf{-1]}}{(\frac{\boldsymbol{f_{mod}}}{\mathbf{5}\boldsymbol{Hz}})^{2}+\left(\frac{\mathbf{4}\boldsymbol{Hz}}{\boldsymbol{f_{mod}}}\right)+\mathbf{1.5}}\boldsymbol{vacil} \qquad (1.27)$$

$\boldsymbol{m}$ is the modulation factor , $\boldsymbol{L_{BBN}}$ is the level of the broad-band noise and $\boldsymbol{f_{mod}}$ is the frequency of modulation.

1.2.2.4 Roughness

As described in 1.2.2.3, roughness is a sensation by amplitude-modulated sound with high modulation frequencies. The reference of roughness is 60dB, 1-kHz tone which is 100% modulated in amplitude at a modulation frequency of 70Hz. The unit of roughness is “asper” and the reference signal is defined as 1 asper.

With the laboratory experiments, a model of roughness is found as equation 1.28.

$$\mathbf{R} = \mathbf{0.3}\frac{\boldsymbol{f_{mod}}}{\boldsymbol{kHz}}\int_{\mathbf{0}}^{\boldsymbol{24Bark}}\frac{\boldsymbol{\Delta L_E(z)dz}}{\boldsymbol{dB/Bark}}\boldsymbol{asper} \tag{1.28}$$

In the equation $\Delta \boldsymbol{L_E}$ is the temporal masking depth and $\boldsymbol{f_{mod}}$ is the frequency of modulation.

1.2.2.5 Annoyance

For the evaluation of sound quality, above four factors are synthesized with each calculation model. The integrated sensation of psychoacoustic factors is psychoacoustic annoyance(PA) which can be quantitively achieved by laboratory experiments.

The quantitative formula of psychoacoustic annoyance is expressed as equation 1.29.

$$\mathbf{PA} = \boldsymbol{N_5}(\mathbf{1} + \sqrt{\boldsymbol{w_s^2} + \boldsymbol{w_{FR}^2}}) \tag{1.29}$$

In the equation, $\boldsymbol{N_5}$ is the percentile loudness in sone ,$\boldsymbol{w_s^2}$ and $\boldsymbol{w_{FR}^2}$ are shown as following equations.

$$\boldsymbol{w_s^2} = (\frac{\boldsymbol{S}}{\boldsymbol{acum}} - \mathbf{1.75}) \cdot \mathbf{0.25}\,\mathbf{log}(\frac{\boldsymbol{N_5}}{\boldsymbol{sone}} + \mathbf{10}) \tag{1.30}$$

$$\text{for } \boldsymbol{S} > \mathbf{1.75}\,\boldsymbol{acum}$$

$$\boldsymbol{w_{FR}^2} = \frac{\mathbf{2.18}}{\left(\frac{\boldsymbol{N_5}}{\boldsymbol{sone}}\right)^{0.4}}(\mathbf{0.4} \cdot \frac{\boldsymbol{F}}{\boldsymbol{vacil}} + \mathbf{0.6} \cdot \frac{\boldsymbol{R}}{\boldsymbol{asper}}) \tag{1.31}$$

S is the sharpness, ***F*** means fluctuation strength and ***R*** represents roughness.

The equation of 1.29 includes all the psychoacoustical factors, yet the results from experiments and predicted values are distinct [25]. From many researches, the most relevant factor regarding annoyance is found to be loudness [30,31,32]. That's why loudness models are designated as ISO standards, while other factors are not. Therefore, in this research, to model the annoyance of combined noise, only the loudness value is chosen for the independent variable. Next session describes the loudness model specifically with two ISO standards.

1.2.3 Loudness Models

1.2.3.1 Zwicker's Loudness Model

In Zwicker's loudness model for stationary sound, the excitation level versus critical-band rate pattern is used as a basis. [24] Total loudness is expressed as an integral of specific loudness which has the unit of sone/Bark. The mathematical expression of Loudness N with the integral of specific loudness over critical-band rate is as in equation 1.32.

$$\mathbf{N} = \int_{0}^{24\,Bark} N'dz \tag{1.32}$$

All critical-band rates are integrated to calculate total loudness.

To derive the specific loudness, Steven's law is adopted that an intensity sensation increases with physical intensity regarding a power law. This also means that a relative change in loudness is proportional to a relative change in intensity. The statement is expressed as equation 1.33 by substituting a loudness into specific loudness, intensity to excitation E and addition of a constant proportionality k.

$$\frac{\Delta N'}{N'} = \mathbf{k}\frac{\Delta E}{E} \text{ or } \frac{\Delta N'}{N' + N'_{gr}} = \mathbf{k}\frac{\Delta E}{E + E_{gr}} \quad (1.33)$$

N'_{gr} and E_{gr} represents the internal noise floors at very low values of $\mathbf{N'}$ and $\mathbf{E}$, which assumed to produce threshold in quiet.

With application of threshold factor, E_{gr}, the excitation producing in quiet by the test-tone excitation, E_{TQ} is calculated as equation 1.34, with s as the ratio between the intensity of the just-noticeable test tone and the intensity of the internal noise appearing within the critical band at the frequency of the test tone.

$$E_{gr} = \frac{E_{TQ}}{s} \quad (1.34)$$

By substitution of equation 1.34 to equation 1.33 and solving the differential equation with boundary condition that excitation equal to zero leads to specific loudness equal to zero, equation 1.35 is derived.

$$\mathrm{N}' = N'_{gr}[\left(1 + \frac{sE}{E_{TQ}}\right)^{k} - 1] \quad (1.35)$$

Application of a reference specific loudness N'_0 transforms the equation 1.35 to 1.36.

$$\mathbf{N'} = N'_0 \left(\frac{E_{TQ}}{sE_0}\right)^k \left[\left(1 + \frac{sE}{E_{TQ}}\right)^k - 1\right] \tag{1.36}$$

The exponent $\mathbf{k}$ is substituted with 0.23, as for the approximation for large values of $\mathbf{E}$ leads to equation 1.37 for which the influence of threshold in quiet is negligible.

$$\mathbf{N'} \sim \left(\frac{E}{E_0}\right) \tag{1.37}$$

The final equation is achieved by the substitution of the threshold factor s =0.5 with the frequencies in the neighborhood of 1kHz and the consideration of boundary condition that a 1-kHz tone with a level of 40 dB produces a total loudness of 1 sone and is expressed as equation 1.38.

$$\mathbf{N'} = 0.08 \left(\frac{E_{TQ}}{E_0}\right)^{0.23} \left[\left(0.5 + 0.5\frac{E}{E_{TQ}}\right)^{0.23} - 1\right] \tag{1.38}$$

The unit of specific loudness is sone/Bark, and total loudness is calculated by integral of equation 1.38 through whole critical bands.

This loudness model of Zwicker is widely used even these days to calculate loudness level of various sounds and even adopted to ISO 532b in 1966.

The loudness model that calculates the loudness of time-varying signal is suggested as “Dynamic Loudness Model(DLM)” [24]. The procedure of DLM is depicted as block diagram in figure 1.1.

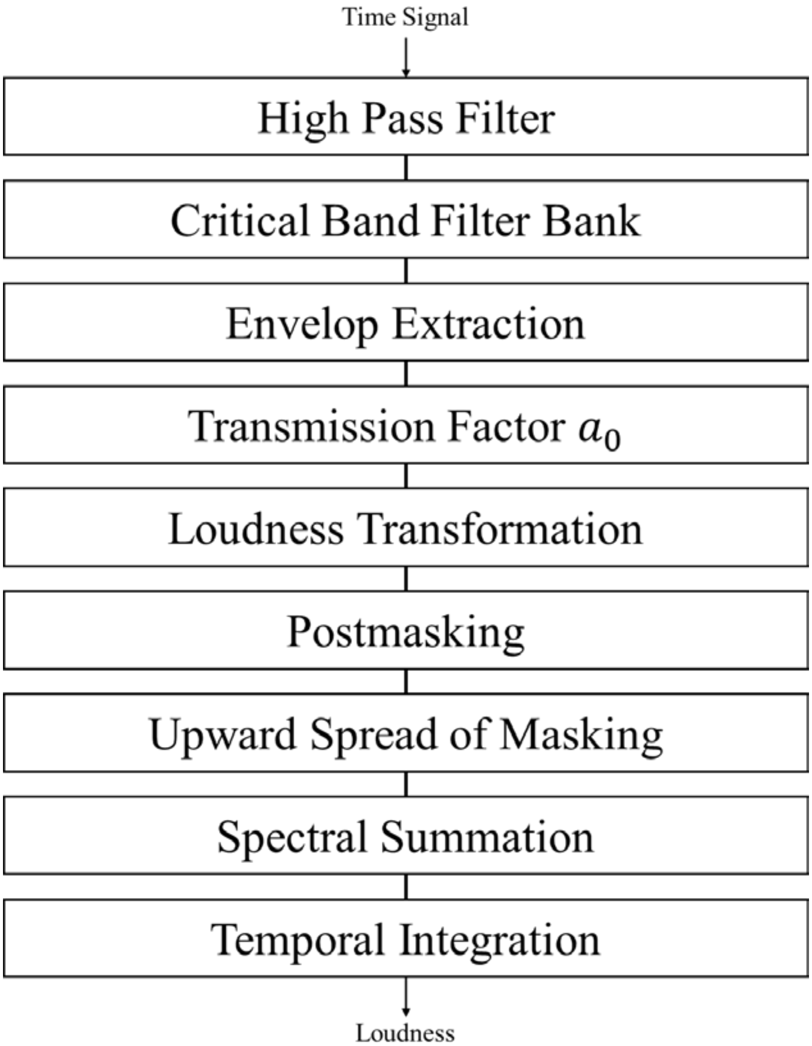

Figure 1.1 Block diagram of the Dynamic Loudness Model (DLM)

The time signal is first passed by a high-pass filter which considers variations of the absolute threshold in the first critical band. A butterworth filter with a slope of 12dB per octave and a cut-off frequency of 50Hz is proposed by the proposer. Next is a critical wide band filter back that performs a spectral analysis that is suitable for the hearing system. In the block “Envelope Extraction, the temporal envelopes of the outputs are extracted by contained window of band pass filters. “Transmission factor $\mathbf{a_0}$ ” block function as described in DIN45631 that represents the transmission between free-field and human hearing system. Next is the “Loudness Transformation” block that calculates specific loudness which describes in equation 1.38. “Postmasking” block simulates the results from Zwicker by a non-linear low pass filter that explains the dependence of postmasking on not only the masker level but also the masker duration. In the block “spread of Masking”, effects of spectral masking as published in DIN

45631 are simulated. “Spectral Summation” block integrates specific loudness along the critical band rate scale. The final block which is “Temporal Upward Integration” function the dependence of loudness on duration with constant sound pressure level.

Two models of loudness with stationary and non-stationary sound are adopted to ISO 532-1:2017. Although many researchers slightly developed these models to improve the predictable accuracy, still these models are frequently used for the calculation of technical sounds

However, the models of loudness by Zwicker only calculate the single sounds that are unable to derive the loudness of combined signals. For the supplementation of it, Moore and Glasberg suggested a new model and it is described in section 1.1.3.2.

1.2.3.2 Moore's Loudness Model

Moore and Glasberg revised the model of loudness by Zwicker to predict the loudness more accurate especially with equal-loudness contours change with sound level [25]. The revisions have been made in the following parts.

1) Modifications in transfer function for the outer and middle ear
2) Changes in calculation of excitation patterns
3) Revisions of relation between specific loudness and excitation for sounds in quiet and in noise.

In this section, each modified part is specifically described.

Figure 1.2 depicts the overall structure of loudness model by Zwicker. The first block of it is a fixed filter for transfer function of outer and middle ear. In Zwicker's model, it is assumed that above 2000Hz, the transfer function has the similar shape to the absolute threshold curve with inverted form due to the assumption of equal sensitivity to all frequency ranges in the inner ear.

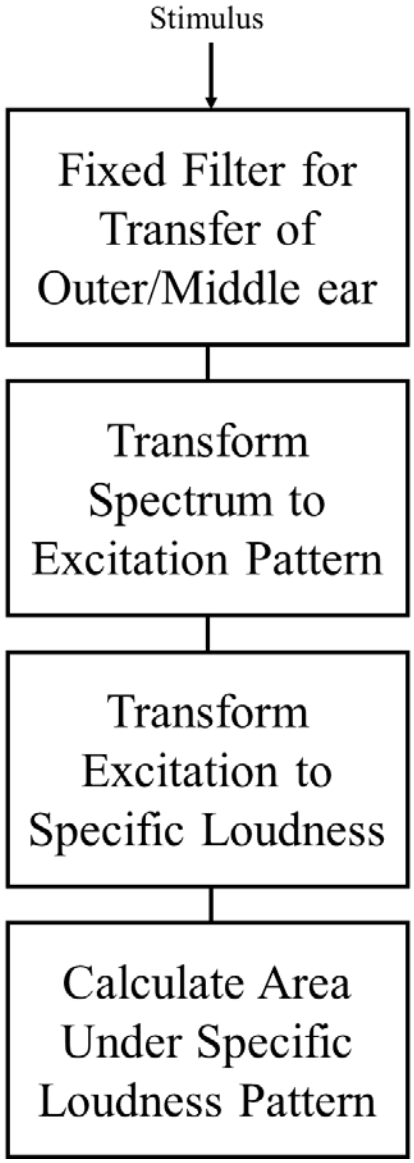

Figure 1.2 Block Diagram of Zwicker's Loudness model

Zwicker also assumed that below 2000Hz, the transmission along the outer and middle ear was constant. At low frequencies the rise of absolute threshold with decreasing frequency is assumed to be caused by increased internal noise. However, recent study revealed that transmission through the outer and middle ear below 1000Hz shows the inverted form of equal-loudness contour roughly at about 100 phon. Moore and Glasberg assumed that above 1000Hz, transmission through the outer and middle ear is the reflected form of the absolute threshold curve. The modified equation to calculate the excitation level at absolute threshold is suggested as equation 1.39.

$$\boldsymbol{LE(thr) = MAF(f) - ELC(f) + 100} \qquad (1.39)$$

$\boldsymbol{LE(thr)}$ represents the excitation level at absolute threshold, *MAF(f)* indicates the absolute threshold curve(minimum audible field) and *ELC(f)* represents the 100-phon equal loudness contour. Moore and Glasberg adopted this newly revised equation to calculate the loudness of a given sound.

Next block of Zwicker's loudness model is the transformation of spectrum to excitation pattern. In Zwicker's model, the masking patterns for narrowband noises are applied to derive the excitation pattern. However, Moore and Glasberg revised this assumption as the masking patterns for narrowband noises could be affected by some factors as beat detection, combination tones and off-frequency listening, in addition to that of strong effect on high-frequency side by the inherent temporal fluctuations in narrow band noise maskers. Instead, the revised model adopted auditory filter shapes that represent frequency selectivity at a particular center frequency to calculate the excitation patterns.

A critical bandwidth related concept, equivalent rectangular bandwidth (ERB) is assumed in modified model at moderate sound levels and it is expressed as equation 1.40.

$$\boldsymbol{ERB = 24.7(4.37F + 1)} \tag{1.40}$$

The unit of *ERB* and *F* are Hz and kHz each. This bandwidth function is similar to critical bandwidth at medium to high frequencies but has lower values below 500Hz. With this relation, excitation patterns for a given sounds is calculated as the pattern of outputs from the auditory filter as a function of center frequency of the filter. The critical band rate scale, or the Bark scale, is then transformed to so called number of ERBs as expressed in equation 1.41.

$$\boldsymbol{Number\ of\ ERBs = 21.4log_{10}(4.37F + 1)} \tag{1.41}$$

Third stage of loudness model by Zwicker is the transformation of excitation to specific loudness, which is the loudness per critical band. From the revised model, specific loudness, N', is depicted with the ERB scale.

Zwicker suggested the relationship between specific loudness and excitation in terms of excitation in power unit, *E*, while Moore and Glasberg introduced an assumption that the specific loudness which is produced by a given amount of excitation is proportional to the internal effect caused by that excitation and it is expressed in equation 1.42 with c and $\boldsymbol{\alpha}$ are constants and $\boldsymbol{\alpha < 1}$.

$$\boldsymbol{N' = \mathbf{c}E^{\alpha}} \tag{1.42}$$

The calculation of loudness is processed with three cases as below.

1. Signal in quiet with $\boldsymbol{E_{SIG} > E_{THRQ}}$
2. Signal in external noise with $\boldsymbol{E_{SIG} \gg E_{THRN}}$
3. Signal in external noise with $\boldsymbol{E_{SIG} \leq E_{THRN}}$

The first case is the sound presented in quiet. Moore and Glasberg assumed the long-term adaptation effect which caused inaudible with internal noise. Modeling of this adaptation is expressed in equation 1.43.

$$\boldsymbol{N' = \mathbf{c}{E_{SIG}}^{\alpha} - A} \tag{1.43}$$

In this expression, $\boldsymbol{E_{SIG}}$ represents the excitation evoked by the signal, and A is a constant. $\mathbf{N'}$ is zero when the signal is at absolute threshold, and $\boldsymbol{E_{SIG} = E_{THRQ}}$ so it leads to equation 1.44 and 1.45.

$$\boldsymbol{A = \mathbf{c}{E_{THRQ}}^{\alpha}} \tag{1.44}$$

$$N' = \mathbf{c}[(E_{SIG})^{\alpha} - (E_{THRQ})^{\alpha}] \qquad (1.45)$$

Substituting all excitations with relative value E_0 for the convenience leads to equation 1.46 and it is the final form of relationship between excitation and specific loudness of sound in quiet.

$$\mathrm{N}' = \mathbf{c}[(E_{SIG}/E_0)^{\alpha} - (E_{THRQ}/E_0)^{\alpha}] \qquad (1.46)$$

Second case is for the signal with background sound. In Zwicker's model, a correction factor was adopted to explain the result that the loudness of a signal increases sharply when the intensity of it is grown from a threshold value to a slight above it. However, Moore and Glasberg introduce a new method for loudness calculation of partially masked signal without adopting correction factor. Equation 1.46 is transformed into equation 1.47 with E_{SIG} and E_{NOISE} as an excitation evoked by the signal and background noise, and N'_{TOT} as the total specific loudness.

$$N'_{TOT} = \mathbf{c}[(\frac{E_{SIG}}{E_0} + \frac{E_{NOISE}}{E_0})^{\alpha} - (\frac{E_{THRQ}}{E_0})^{\alpha}] \qquad (1.47)$$

It is assumed that $N'_{TOT} = N'_{SIG} + N'_{NOISE}$.

N'_{SIG} is zero when the signal is at its masked threshold with excitation E_{THRN} and it leads to equation 1.48.

$$N'_{NOISE} = \mathbf{c}[(\frac{E_{THRN}}{E_0} + \frac{E_{NOISE}}{E_0})^{\alpha} - (\frac{E_{THRQ}}{E_0})^{\alpha}] \qquad (1.48)$$

For the case 2, when $\boldsymbol{E'_{SIG} \gg E'_{THRN}}$, that means a signal centered in narrowband noise is above its masked threshold, $\boldsymbol{N'_{SIG}}$ is approached as $\mathbf{c}[(\boldsymbol{E_{SIG}/E_0})^{\boldsymbol{\alpha}} - (\boldsymbol{E_{THRQ}/E_0})^{\boldsymbol{\alpha}}]$ and it leads to equation 1.49.

$$\begin{aligned} \boldsymbol{N'_{NOISE}} &= \boldsymbol{N'_{TOT} - N'_{SIG}} \\ &= \mathbf{c}[(\frac{\boldsymbol{E_{SIG}}}{\boldsymbol{E_0}} + \frac{\boldsymbol{E_{NOISE}}}{\boldsymbol{E_0}})^{\boldsymbol{\alpha}} - (\frac{\boldsymbol{E_{SIG}}}{\boldsymbol{E_0}})^{\boldsymbol{\alpha}}] \end{aligned} \tag{1.49}$$

Transformation of equation 1.49 to 1.50 leads to introduction of a function *B* whose value varies from zero when $\boldsymbol{E_{SIG} \leq E_{THRN}}$ which is case 3, and to unity when $\boldsymbol{E_{SIG} \geq E_{THRN}}$ for the case 2.

$$\begin{aligned} \boldsymbol{N'_{NOISE}} = \mathbf{c}[(\frac{\boldsymbol{E_{SIG}}}{\boldsymbol{E_0}} + \frac{\boldsymbol{E_{NOISE}}}{\boldsymbol{E_0}})^{\boldsymbol{\alpha}} - \boldsymbol{B}\left(\frac{\boldsymbol{E_{SIG}}}{\boldsymbol{E_0}}\right)^{\boldsymbol{\alpha}} \\ -(\mathbf{1} - \boldsymbol{B})\left(\frac{\boldsymbol{E_{THRQ}}}{\boldsymbol{E_0}}\right)^{\boldsymbol{\alpha}}] \end{aligned} \tag{1.50}$$

The function *B* is assumed that varies continuously and smoothly between zero to unity and the simplest form of it when $\boldsymbol{E_{SIG} \geq E_{THRN}}$ is $\mathbf{B = 1 -} (\boldsymbol{E_{THRN}/E_{SIG}})$. From this it leads to equation 1.51.

$$\begin{aligned} \boldsymbol{N'_{SIG}} &= \boldsymbol{N'_{TOT} - N'_{NOISE}} \\ &= \mathbf{c}\left(\mathbf{1} - \frac{\boldsymbol{E_{THRN}}}{\boldsymbol{E_0}}\right) \times [\left(\frac{\boldsymbol{E_{SIG}}}{\boldsymbol{E_0}}\right)^{\boldsymbol{\alpha}} - \left(\frac{\boldsymbol{E_{THRQ}}}{\boldsymbol{E_0}}\right)^{\boldsymbol{\alpha}}] \end{aligned} \tag{1.51}$$

For the convenience, substituting $\boldsymbol{E_{THRN}}$ into $\boldsymbol{kE_{NOISE}}$ with k as the ratio of signal power to noise power within the ERB near the signal frequency for a signal at threshold leads to the final form expressed as equation 1.52.

$$\boldsymbol{N'_{SIG}} = \mathbf{c}\left(\mathbf{1} - \frac{\mathrm{k}\boldsymbol{E_{NOISE}}}{\boldsymbol{E_0}}\right) \times \left[\left(\frac{\boldsymbol{E_{SIG}}}{\boldsymbol{E_0}}\right)^{\boldsymbol{\alpha}} - \left(\frac{\boldsymbol{E_{THRQ}}}{\boldsymbol{E_0}}\right)^{\boldsymbol{\alpha}}\right] \qquad (1.52)$$

The predictability of this revised model is described in [25] and it shows higher accuracy than Zwicker's model for calculation of loudness.

1.2.3.3 Moore's Partial Loudness Model

Moore's partial loudness model is an advanced model than the method from section 1.1.3.2 that calculates the partial loudness of combined noises with each noise source. The procedures for calculation of loudness are same as figure 1.2 but details of them are revised. First, the loudness model for sound in quiet with stationary signal is introduced [26].

Steps for transfer functions of eardrum and middle ear and transformation of spectrum to excitation pattern are identical with section 1.1.3.2. The modification is conducted in the stage of transformation of excitation pattern to specific loudness.

The relation between specific loudness and the excitation is as same as equation 1.42. As the transfer function of basilar membrane grows steeper and approaches linearity in the vicinity of the absolute threshold for low sound levels, equation 1.42 is modified to have increasing slope, as equation 1.53.

$$\boldsymbol{N}' = \boldsymbol{C}[(\boldsymbol{E_{SIG}} + \boldsymbol{A})^{\boldsymbol{\alpha}} - \boldsymbol{A}^{\boldsymbol{\alpha}}] \tag{1.53}$$

A is a constant with frequency dependent.

The gain by the cochlear amplifier decreases al low frequency ranges and it causes an increment in the excitation required at absolute threshold $\boldsymbol{E_{THRQ}}$ and also produces an increase in the slope of transfer function of basilar membrane which causes the increase of $\boldsymbol{\alpha}$. For the application of these effects, low level gain of cochlear amplifier at a specific frequency which is relative to the gain at 500Hz and above, *G*, is suggested and the equation 1.53 is modified as equation 1.54.

$$\boldsymbol{N}' = \boldsymbol{C}[(\boldsymbol{G}\boldsymbol{E_{SIG}} + \boldsymbol{A})^{\boldsymbol{\alpha}} - \boldsymbol{A}^{\boldsymbol{\alpha}}] \tag{1.54}$$

When the excitation level is 100dB or above, it is assumed that cochlear amplifier has no effect, so that specific loudness should be independent of *G* when $\boldsymbol{E_{SIG}}$ is $\boldsymbol{10^{10}}$, which is 100dB. It results in 4.62 for $\boldsymbol{N}'$. Also, it is assumed that the maximum of specific loudness for a sinusoidal signal is independent of frequency at the absolute threshold, and it leads to equation 1.55.

$$\begin{aligned}\boldsymbol{N'_{ABS}} &= \mathbf{C}[(\mathbf{G}\boldsymbol{E_{THRQ}} + \boldsymbol{A})^{\boldsymbol{\alpha}} - \boldsymbol{A}^{\boldsymbol{\alpha}}] = \boldsymbol{constant} \\ &= \mathbf{0.00537}\end{aligned} \tag{1.55}$$

From equation 1.55, it shows difference from Zwicker's loudness model that specific loudness never becomes zero even for small value of signal. In addition, the slope of relation between specific loudness and $\boldsymbol{E_{SIG}}$ in the range of absolute threshold is lower than the earlier model in section 1.2.3.2 and Zwicker's model, which improves the accuracy of predictions for the change of loudness with levels just above the absolute threshold.

To accommodate the effect that when $\boldsymbol{E_{SIG}}$ decreases below $\boldsymbol{E_{THRQ}}$, the specific loudness also decreases more rapidly that equation 1.54, considering the effects of neural activity, equation 1.54 is modified to equation 1.56 in the case of $\boldsymbol{E_{SIG} < E_{THRQ}}$

$$\boldsymbol{N' = C(\frac{2E_{SIG}}{E_{SIG} + E_{THRQ}})^{1.5}[(GE_{SIG} + A)^{\alpha} - A^{\alpha}]} \qquad (1.56)$$

For the case of extremely large value of $\boldsymbol{E_{SIG}}$, which is $\boldsymbol{E_{SIG} > 10^{10}}$, the equation 1.57 is suggested.

$$\boldsymbol{N' = C(\frac{E_{SIG}}{1.04 \times 10^{6}})^{0.5}} \qquad (1.57)$$

Then the equation 1.54 is applied for the case of $\boldsymbol{E_{THRQ} \ll E_{SIG} \ll 10^{10}}$.

For the sound with background noise, the loudness models are developed with five different cases.

The first case is when $\boldsymbol{E_{SIG} > E_{THRQ}}$ and $\boldsymbol{E_{SIG} + E_{NOISE} < 10^{10}}$. The equation 1.54 is modified as equation 1.58.

$$\begin{aligned} \boldsymbol{N'_{TOT}} &= \mathbf{C}\{[(\boldsymbol{E_{SIG}} + \boldsymbol{E_{NOISE}})\boldsymbol{G} + \boldsymbol{A}]^{\boldsymbol{\alpha}} - \boldsymbol{A}^{\boldsymbol{\alpha}}\} \\ &= \boldsymbol{N'_{SIG}} + \boldsymbol{N'_{NOISE}} \end{aligned} \tag{1.58}$$

The specific loudness for the background noise with excitation above threshold is expressed as equation 1.59.

$$\boldsymbol{N'_{NOISE}} = \mathbf{C}[(\boldsymbol{E_{NOISE}} + \boldsymbol{A})^{\boldsymbol{\alpha}} - \boldsymbol{A}^{\boldsymbol{\alpha}}] \tag{1.59}$$

Then the specific loudness of a target signal is derived by substituting equation 1.59 to 1.58, and it leads to equation 1.60.

$$\begin{aligned} \boldsymbol{N'_{SIG}} = \mathbf{C}\{[(\boldsymbol{E_{SIG}} + \boldsymbol{E_{NOISE}})\boldsymbol{G} + \boldsymbol{A}]^{\boldsymbol{\alpha}} - \boldsymbol{A}^{\boldsymbol{\alpha}}\} \\ - \ \mathbf{C}[(\boldsymbol{E_{NOISE}} + \boldsymbol{A})^{\boldsymbol{\alpha}} - \boldsymbol{A}^{\boldsymbol{\alpha}}] \end{aligned} \tag{1.60}$$

Moore and Glasberg introduce a factor B which is expressed as equation 1.61.

$$\mathbf{B} = \frac{[(\boldsymbol{E_{THRN}} + \boldsymbol{E_{NOISE}})\boldsymbol{G} + \boldsymbol{A}]^{\boldsymbol{\alpha}} - (\boldsymbol{E_{THRQ}}\boldsymbol{G} + \boldsymbol{A})^{\boldsymbol{\alpha}}}{(\boldsymbol{E_{NOISE}}\boldsymbol{G} + \boldsymbol{A})^{\boldsymbol{\alpha}} - \boldsymbol{A}^{\boldsymbol{\alpha}}} \tag{1.61}$$

Applying this suggested factor to equation 1.61 leads to equation 1.62.

$$\begin{aligned} \boldsymbol{N'_{SIG}} = \mathbf{C}\{[(\boldsymbol{E_{SIG}} + \boldsymbol{E_{NOISE}})\boldsymbol{G} + \boldsymbol{A}]^{\boldsymbol{\alpha}} - \boldsymbol{A}^{\boldsymbol{\alpha}}\} \\ - \mathbf{C}\{[(\boldsymbol{E_{THRN}} + \boldsymbol{E_{NOISE}})\boldsymbol{G} + \boldsymbol{A}]^{\boldsymbol{\alpha}} \\ - (\boldsymbol{E_{THRQ}}\boldsymbol{G} + \boldsymbol{A})^{\boldsymbol{\alpha}}] \end{aligned} \tag{1.62}$$

It is assumed that when the signal is at masked threshold, the peak excitation, $\boldsymbol{E_{THRN}}$ is identical with $\mathbf{K}\boldsymbol{E_{NOISE}} + \boldsymbol{E_{THRQ}}$ and K represents the signal to noise ratio of auditory filter. Substitution of $\boldsymbol{E_{THRN}}$ is equation 1.62 leads to equation 1.63.

$$\begin{aligned} \boldsymbol{N'_{SIG}} &= \mathbf{C}\{[(\boldsymbol{E_{SIG}} + \boldsymbol{E_{NOISE}})\boldsymbol{G} + \boldsymbol{A}]^{\boldsymbol{\alpha}} - \boldsymbol{A}^{\boldsymbol{\alpha}}\} \\ &\quad - \mathbf{C}\{[(\boldsymbol{E_{NOISE}}(\mathbf{1} + \boldsymbol{K}) + \boldsymbol{E_{THRQ}})\boldsymbol{G} + \boldsymbol{A}]^{\boldsymbol{\alpha}} \\ &\quad - (\boldsymbol{E_{THRQ}}\boldsymbol{G} + \boldsymbol{A})^{\boldsymbol{\alpha}}] \end{aligned} \tag{1.63}$$

The second case is for the signal above the masked threshold, which is $\boldsymbol{E_{SIG}} \gg \boldsymbol{E_{THRN}}$. When the signal is much louder than the background sound, the effect of $\boldsymbol{E_{NOISE}}$ almost disappears and to consider this effect, new factor $\boldsymbol{E_{THRN}}/\boldsymbol{E_{SIG}}$ is suggested. With new factor adopted, equation 1.63 is modified as equation 1.64.

$$\begin{aligned} \boldsymbol{N'_{SIG}} &= \mathbf{C}\{[(\boldsymbol{E_{SIG}} + \boldsymbol{E_{NOISE}})\boldsymbol{G} + \boldsymbol{A}]^{\boldsymbol{\alpha}} - \boldsymbol{A}^{\boldsymbol{\alpha}}\} \\ &\quad - \mathbf{C}\big\{\big[(\boldsymbol{E_{NOISE}}(\mathbf{1} + \boldsymbol{K}) + \boldsymbol{E_{THRQ}}\big)\boldsymbol{G} + \boldsymbol{A}\big]^{\boldsymbol{\alpha}} \\ &\quad - \big(\boldsymbol{E_{THRQ}}\boldsymbol{G} + \boldsymbol{A}\big)^{\boldsymbol{\alpha}}\}\Big(\frac{\boldsymbol{E_{THRN}}}{\boldsymbol{E_{SIG}}}\Big)^{\mathbf{0.3}} \end{aligned} \tag{1.64}$$

The exponent 0.3 is achieved from empirical data and it is the complete form for the case $\boldsymbol{E_{SIG}} \gg \boldsymbol{E_{THRN}}$ and $\boldsymbol{E_{SIG}} + \boldsymbol{E_{NOISE}} \ll \mathbf{10^{10}}$.

For the third case when $\boldsymbol{E_{SIG}} < \boldsymbol{E_{THRN}}$, with the consideration of slope for decreasing $\boldsymbol{E_{SIG}}$ with $\boldsymbol{E_{THRN}}$, the final form of relation is expressed as equation 1.65.

$$N'_{SIG} = C\left(\frac{2E_{SIG}}{E_{SIG}+E_{THRN}}\right)^{1.5}\left\{\frac{\left(E_{THRQ}G+A\right)^{\alpha} -}{\left[\left(E_{NOISE}(1+K)+E_{THRQ}\right)G+A\right]} \right. \times \{[(E_{SIG}+E_{NOISE})G+A]^{\alpha}-(E_{NOISE}G+A)^{\alpha} \quad (1.65)$$

The last case for $E_{SIG} \gg E_{THRN}$ and $E_{SIG}+E_{NOISE} > 10^{10}$ is considered and with same method as adopted in the third case, it is expressed as equation 1.66.

$$N'_{SIG} = C_2(E_{SIG}+E_{NOISE})^{0.5} - C_2\{\left[(E_{NOISE}(1+K)+E_{THRQ}\right]^{0.5} - \left(E_{THRQ}G+A\right)^{\alpha} + A^{\alpha}\}(\frac{E_{THRN}}{E_{SIG}})^{0.3} \quad (1.66)$$

C_2 is identical with $C/(1.04 \times 10^{6})^{0.5}$.

Finally, the case for $E_{SIG} < E_{THRN}$ and $E_{SIG}+E_{NOISE} > 10^{10}$ is expressed as equation 1.67.

$$N'_{SIG} = C\left(\frac{2E_{SIG}}{E_{SIG}+E_{THRN}}\right)^{1.5}\left\{\frac{\left(E_{THRQ}G+A\right)^{\alpha} - A^{\alpha}}{\left[E_{NOISE}(1+K)+E_{THRQ}]^{0.5}\right]-(I} \right. \times [(E_{SIG}+E_{NOISE})^{0.5}-(E_{NOISE})^{0.5}] \quad (1.67)$$

Equation 1.63, 1.64, 1.65, 1.66, and 1.67 are the final forms of partial loudness model of stationary signal with each designated situation.

For the calculation of loudness for time-varying signal, temporal integration of instantaneous loudness is conducted with the former introduced methods [27]. The averaging method of for instantaneous loudness is similar to an automatic gain control which has attack time $\boldsymbol{T_a}$ and release time $\boldsymbol{T_r}$. The short-term loudness with averaged every 1ms to the nth time frame is defined as $\boldsymbol{S'_n}$ and with the time frame n-1 is assigned as $\boldsymbol{S'_{n-1}}$.

If $\boldsymbol{S_n} > \boldsymbol{S'_{n-1}}$ the corresponding short-term loudness is defined as equation 1.68.

$$\boldsymbol{S'_n = \alpha_a S_n + (1 - \alpha_a) S'_{n-1}} \tag{1.68}$$

$\boldsymbol{\alpha_a}$ is a constant with defined as equation 1.69.

$$\boldsymbol{\alpha_a = 1 - e^{-T_i/T_a}} \tag{1.69}$$

$\boldsymbol{T_i}$ is the time interval between continuous factor of the instantaneous loudness.

If $\boldsymbol{S_n \leq S'_{n-1}}$, the short-term loudness is defined as equation 1.70.

$$\boldsymbol{S'_n = \alpha_r S_n + (1 - \alpha_r) S'_{n-1}} \tag{1.70}$$

$\boldsymbol{\alpha_r}$ corresponds to equation 1.71.

$$\boldsymbol{\alpha_r = 1 - e^{-T_i/T_r}} \tag{1.71}$$

The $\boldsymbol{\alpha_a}$ and $\boldsymbol{\alpha_r}$ is suggested to 0.045 and 0.02 by Moore and Glasberg.

For the calculation of long-term loudness, same method is adopted from the model of short-term loudness with modified coefficients.

Long-term loudness with nth time frame is defined as $\boldsymbol{S''_n}$ and if $\boldsymbol{S'_n} > \boldsymbol{S''_{n-1}}$, then the long-term loudness is calculated as equation 1.72.

$$\boldsymbol{S''_n = \alpha_{al} S'_n + (1 - \alpha_{al}) S''_{n-1}} \tag{1.72}$$

$\boldsymbol{\alpha_{al}}$ corresponds to the attack time of the long-term loudness averager.

If $\boldsymbol{S'_n \leq S''_{n-1}}$, the long-term loudness is defined as equation 1.73.

$$\boldsymbol{S''_n = \alpha_{rl} S'_n + (1 - \alpha_{rl}) S''_{n-1}} \tag{1.73}$$

The coefficients $\boldsymbol{\alpha_{al}}$ and $\boldsymbol{\alpha_{rl}}$ is set to 0.01 and 0.0005 by the proposers. In this research, as the loudness values of nonstationary signal vary with time, the maximum of long-term loudness is selected for the representative value as it is reasonable to stand for the loudness value in real situation and also for the suggestion by Moore and Glasberg.

1.3 Research Objectives

Two models of combined noise annoyance with binaural inhibition are suggested regarding noise exposure time. Short-term annoyance model for single flyover of aircraft and long-term annoyance model for noise exposure more than a year are proposed in this research. Suggested models are simple to adopt in noise mapping program so that annoyance maps which are advanced form compared to noise maps are added.

Chapter 2 describes the newly suggested model which calculates the partial loudness of combined noises incorporating binaural inhibition. For the laboratory test, stimuli of aircraft and road traffic noise are recorded and conducted the experiment in an anechoic chamber. By the comparison of test results and calculated values from partial loudness model with binaural inhibition, the model is validated for the adoption in following modeling.

In chapter 3, experiments and modeling procedures of short-term annoyance for combined noises from aircraft and road traffic noise are described. With the help of laboratory test, annoyance of combined noise with aircraft and road traffic noise are rated by test subjects. In the modeling procedures, independent variable that causes a dependent value, annoyance, is chosen as loudness, a psychoacoustic factor. As the annoyance value is also a psychoacoustic value, loudness is better relevant to it than other physical factors. To calculate the loudness of combined noises, partial loudness model with binaural inhibition is first adopted to environmental sounds in this research. Partial loudness model calculates each loudness value that comprise the combined noise. By calculating the partial loudness of each stimuli and executing the logistic regression with annoyance ratings, short-term annoyance model of combined noise by aircraft and road traffic noise is deduced.

In chapter 4, annoyance caused by residents who have lived in the environment of combined noise exposure which evokes long-term annoyance is investigated. By the field survey and noise mapping in research area, noise levels of residents and annoyance ratings of combined noise by aircraft and road traffic noise are acquired. With these collected data, long-term annoyance model of combined noise by aircraft and road traffic noise is deduced as the same method conducted in chapter 3.

Annoyance mapping procedures and the map of annoyance in research area are introduced in chapter 5. By the annoyance map, the degree of annoyance is recognizable at a glance. Also, background noise effect of combined noise is also presented in annoyance map that former noise maps were unable to show.

Chapter 6 concludes the whole researches and includes the significances of these studies.

Chapter. 2

Development of Partial Loudness Model with Binaural Inhibition

In chapter 1, the partial loudness model for time-varying sounds with combined noises was introduced. It calculates the value of loudness with the effect of background noise so that contribution of each noise source is considered. However, it only represents the loudness of single channel of noise so that in order to derive the partial loudness of binaural hearing, doubling the loudness should be conducted for two ears.

Many researches have investigated to reveal the effect of binaural hearing. Kim et al. executed the laboratory test for the comparison of monaural and binaural listening to show that annoyance from the single and dummy head results in different tendency with increasing noise level yet not as twice [16]. It means that listening the noise from two ears is not as same as the hearing the two single channels.

In this section, binaural effect on loudness is first covered and application to the partial loudness model is conducted to develop the former suggested partial loudness model. Next, newly designed partial loudness model is validated with laboratory test for evaluation of predictability on transportation noises.

2.1 Sound Pressure Comparison between Monaural and Binaural Sound

In this section, sound pressure between monaural and binaural sounds are compared from physical point of view [28]. Due to a monopole source, the sound pressure at receiver point R is expressed as equation 2.1.

$$\boldsymbol{p(t)=\left(\frac{\rho_0}{4\pi r}\right)\frac{\partial}{\partial t}\left[Q\left(t-\frac{r}{c}\right)\right]=\left(\frac{\rho_0}{4\pi r}\right)a\left(t-\frac{r}{c}\right)} \tag{2.1}$$

In the equation, r is the radial distance between source and receiver, c is the speed of sound in the condition of air, ρ_0 is the air density, Q is the volume velocity and a is the rate of change of the volume velocity which is the volume acceleration of the source.

By the linear superposition of each monopole, the sound pressure from a group of monopoles are deduced from equation 2.1 and it is calculated as equation 2.2.

$$\boldsymbol{p(t)=\sum_{n=1}^{N}p_n(t)=\sum_{n=1}^{N}\left(\frac{\rho_0}{4\pi r}\right)a_n\left(t-\frac{r_n}{c}\right)} \tag{2.2}$$

$\boldsymbol{a_n}$ is the $\boldsymbol{n}$th source's volume acceleration and $\boldsymbol{r_n}$ is the distance between receiver point R and $\boldsymbol{n}$th source. Equation 2.2 derives the sound pressure of monaural signal at receiver point located in the center of a head of observer.

For the application of binaural effect, Head Related Transfer Functions(HRTFs) is necessary to be considered. HRTFs include time, frequency, angle and distance from receiver. By the convolution between monaural signal and Head Related Impulse Response(HRIR), binaural signal of sound is found. The contribution of sound pressure at the left ear from the $\boldsymbol{n}$th monopole source is expressed as equation 2.3.

$$\boldsymbol{p_{Ln}(t) = \int_0^\infty H_L(\theta_n, \varphi_n, \tau)\, p_n(t-\tau) d\tau} \tag{2.3}$$

$\boldsymbol{H_L}$ is the HRIR of left ear and $\boldsymbol{\tau}$ is a temporal variable. The contribution of right ear is as same as equation 2.3 with different HRIR.

For the computer calculation, equation 2.3 is discretized as equation 2.4.

$$\boldsymbol{p_{Ln}[i] = \sum_{j=0}^{M-1} H_L[\theta_n, \varphi_n, j]\, p_n[i-j]} \tag{2.4}$$

$\boldsymbol{M}$ is the number of taps involving HRIR finite impulse response(FIR) filter and $\boldsymbol{i}$ is the $\boldsymbol{i}$th discrete time step. By summing every pressure contribution of monopole from left ear, sound pressure of left ear is shown as equation 2.5.

$$\boldsymbol{p_L[i] = \sum_{n=1}^{N} p_{Ln}[i] = \sum_{n=1}^{N} \sum_{j=0}^{M-1} H_L\,[\theta_n, \varphi_n, j] p_n[i-j]} \tag{2.5}$$

The final form of equation implies the binaural effects which includes the reflection, diffraction and refraction of the sound by pinna and other bodies. As can be seen from the equation, binaural sound pressure is different from monaural signal and reflects the real hearing situations. In this research, binaural effect is implemented to former loudness model for the calculation of partial loudness with binaural inhibition.

2.2 Loudness Model with Binaural Inhibition

Moore and Glasberg developed the former loudness model which is introduced in section 1.2.2.3 to calculate the partial loudness. In former models, binaural effect was not considered, doubling the monaural loudness values was the only method. However, comparisons of experimental results show that it does not coincide with the predicted values. Specifically, laboratory test results are less than the calculated loudness values. Moore referred to this effect as "binaural inhibition".

Binaural inhibition is the concept that the sound heard from one ear reduces the internal response of the signal at the other ear. The processes for the calculation of loudness with each ear incorporating binaural inhibition is shown in figure 2.1 [29].

Compared to figure 1.3, the loudness calculations are conducted with each ear. Inhibition of each ear by the effect of the other ear is included. Also, the calculation of smoothed loudness is implemented in this model. Other stages are as same as the model of section 1.2.3.3.

Smoothed short-term specific loudness is calculated as equation 2.6

$$\boldsymbol{N'_L(i)_{smoothed}} = \sum_{\boldsymbol{D_i=-18}}^{\boldsymbol{D_i=+18}} \boldsymbol{N'_L(i-D_i)}\mathbf{exp}[-(\boldsymbol{BD_i})^{\mathbf{2}}] \tag{2.6}$$

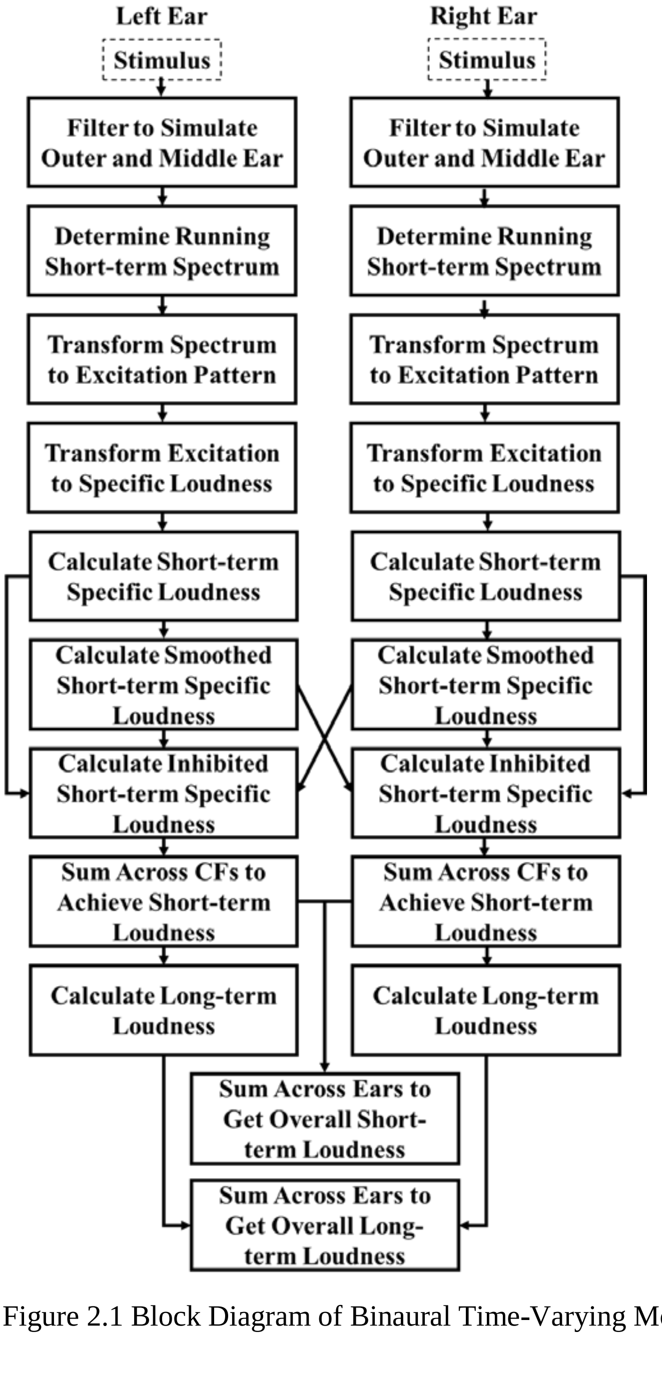

Figure 2.1 Block Diagram of Binaural Time-Varying Model

$\boldsymbol{N'_L(i)}$ represents the smoothed short-term specific loudness of left ear and $\boldsymbol{D_i}$ is the deviation from the given $\boldsymbol{i}$ and $\boldsymbol{B}$ is a factor that determines the degree of spread of inhibition along the ERB scale which is set to 0.08 from the experimental data fitting. The smoothed loudness for the right ear is calculated in same way.

By the application of smoothed loudness, the inhibited short-term specific loudness is calculated as equation 2.7.

$$\boldsymbol{INH_{IPSI}(i)} = \frac{\mathbf{2}}{\left[\mathbf{1} + \left\{\mathbf{sech}\left(\frac{\boldsymbol{N'_{CONTRA}(i)_{smoothed}}}{\boldsymbol{N'_{IPSI}(i)_{smoothed}}}\right)\right\}^{\boldsymbol{\theta}}\right]} \qquad (2.7)$$

$\boldsymbol{INH_{IPSI}(i)}$ is the value that the short-term specific loudness evoked by the sound at one ear is reduced with inhibition by the signal from the contralateral ear. $\boldsymbol{N'_{CONTRA}}$ and $\boldsymbol{N'_{IPSI}}$ are the smoothed short-term specific loudness of contralateral and ipsilateral ears, and $\boldsymbol{\theta = 1.598}$. Equation 2.7 is applied to processes of former loudness calculation to achieve the loudness values with binaural inhibition.

2.3 Partial Loudness Model with Binaural Inhibition

From the ideas of partial loudness model and loudness incorporating binaural inhibition, partial loudness model with binaural inhibition is newly suggested in this research. The whole processes are depicted as block diagram in figure 2.2.

Most of the procedures are similar as those of partial loudness mode, yet smoothed short-term specific partial loudness calculation and inhibited short-term specific partial loudness blocks are added. Also, the calculations are conducted for each ear so that total loudness with binaural inhibition is deduced by the sum of loudness from each ear.

2.4 Validation of the Model

Before the application of partial loudness model with binaural inhibition which is newly developed in this study, validation of this model should be done for the evaluation of suitability in environmental noises and further applications. For the purpose of this research, aircraft and road traffic noise are selected for the representative environmental noises.

2.4.1 Jury Test

An experiment is planned for comparing the loudness of aircraft noise in quiet and with background noise with adaptive procedure method. In this research, background noise is selected with road traffic noise.

The experiment is conducted in anechoic chamber, as shown in figure 2.3, with the ambient sound level of about 20dBA and the cut-off frequency of 200Hz.

Total fourteen subjects, with three women and eleven men, were selected

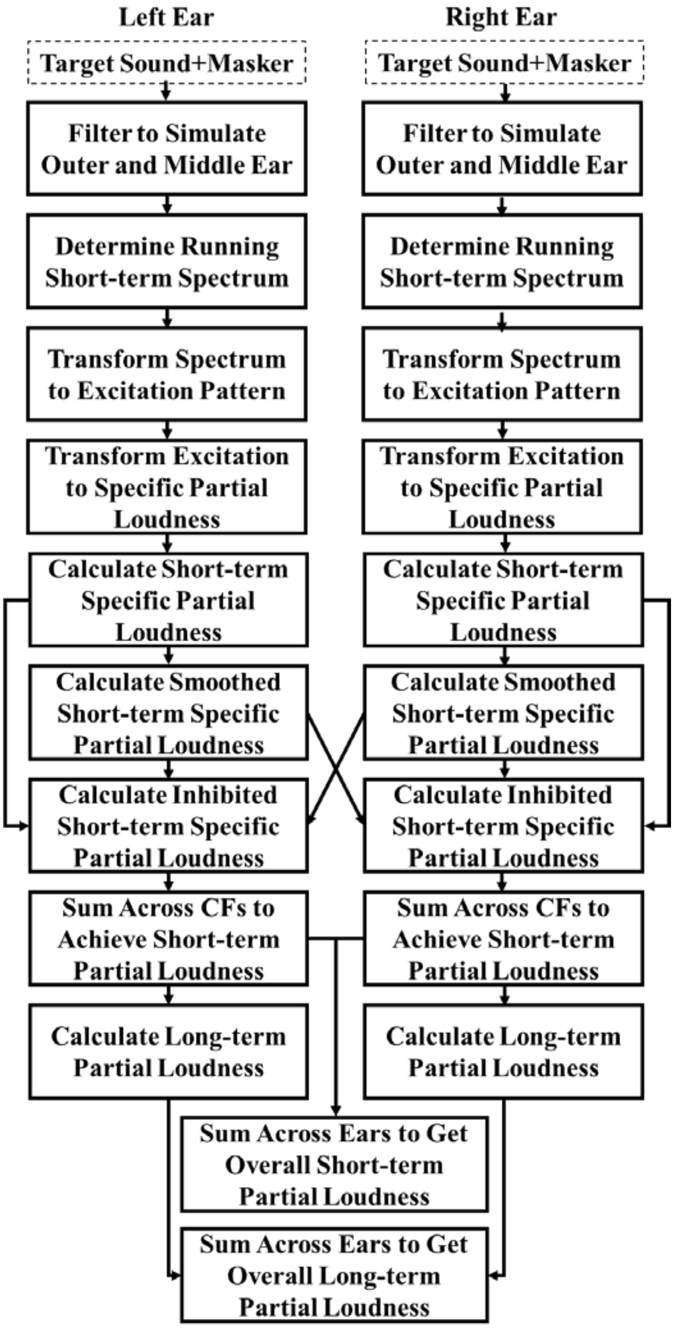

Figure 2.2 Block Diagram of Partial Loudness Model with Binaural Inhibition

Figure 2.3 Anechoic Chamber for Laboratory Test

Figure 2.4 Head and Torso Simulator for Binaural Recording

for validation test and before the main test, screening test was preceded to check the subjects' hearing issues, and which turns out all the subjects have normal hearing. The range of age is between 22 to 30 with average 28.7.

2.4.2 Stimuli

To achieve the experimental stimuli, recordings of aircraft and road traffic noise were conducted. For binaural recording, HATS(Head and Torso Simulator) by B&K is used to measure the recordings of binaural sound as shown in figure 2.4. HATS has two channels of microphone in the position of ear so that it is capable of binaural recording. Also, it has pinna-shaped rubber forms and body-shaped torso to duplicate the diffraction of sound by pinna and body. Aircraft noise was measured and recorded near Gimpo airport in South Korea. Civil aircraft flyover noise was recorded below the route of aircraft flyover. Total 5 aircraft flyover noises were recorded, and one representative flyover noise is selected as the test stimulus.

Road traffic noise was achieved from the 8-lane road in Seoul. The recording period is from 15:00 to 15:30 to avoid heavy traffic. Total 30 minute of recoding was done and from the achieved data, and from it 20 seconds of normal recoding period was selected for the experimental stimulus.

The spectral and loudness characteristics of recorded sounds of aircraft and road traffic noise are depicted in figure 2.5 with the aircraft and road traffic

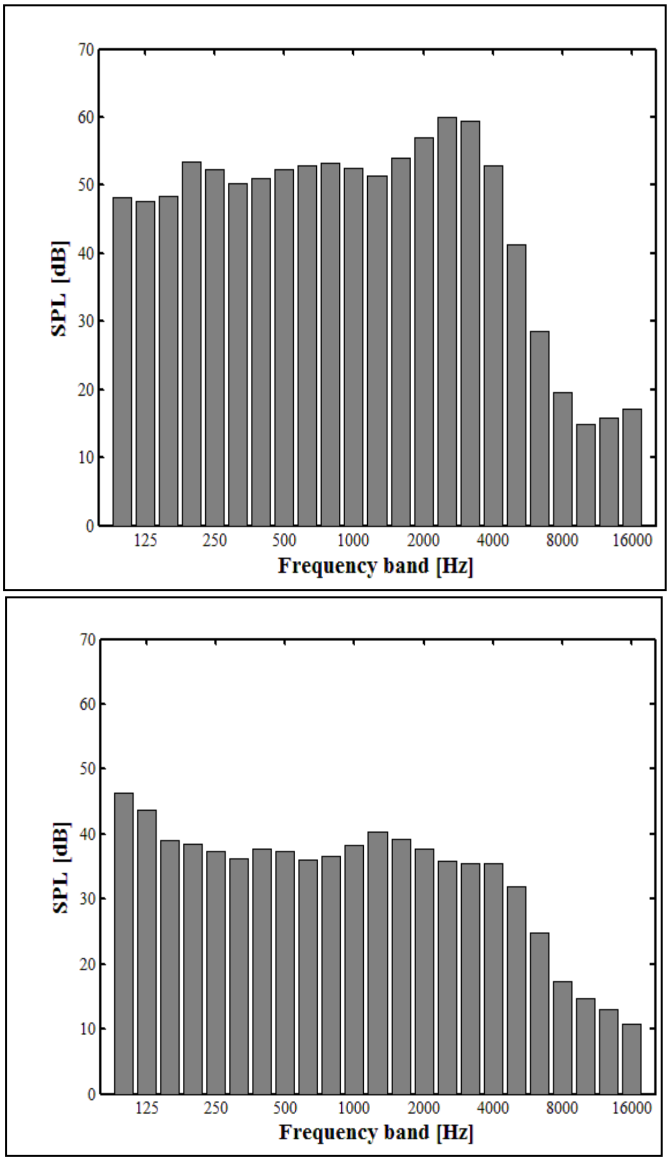

Figure 2.5 One-third Octave Band of Test Stimuli (Upper: Aircraft, Lower: Road Traffic Noise)

noise adjusted to 60dB $L_{A_{eq}}$. As it is shown in the figure, aircraft noise has high frequency components while road traffic noise has broadband property. The recorded sounds are employed not only in this validation, but also for the modeling of short-term annoyance in chapter 3.

The stimuli of aircraft sound are adjusted to 68, 73, 78 dBA in Leq and the sounds of road traffic noise are 55, 65, 75 dBA in Leq. The loudness of aircraft noise with 68dB L_{eq} is shown in figure 2.6 to 2.10. Figure 2.6 shows the amplitude, instantaneous loudness level(ILL), short-term loudness level(STL) and long-term loudness level(LTL) of aircraft noise with 68dB in left ear. The maximum of STL is 75.4 phon and the maximum of LTL is 74.6 phon. Figure 2.7 shows the same loudness of aircraft noise with the unit of sone. The maximum STL is 11.7 sone and the maximum LTL is 11.0 sone. Figure 2.8 shows the sensory time-frequency representation of the left ear from aircraft noise. It represents the specific loudness of each ERB with respect to time and center frequency of ERB. Figure 2.9 to 2.11 show the loudness values of road traffic noise with 55dB in left ear. In figure 2.9 and 2.10, it is shown that maximum STL of road traffic noise is 57.6 phon and 3.6 sone and the maximum LTL is 57.3 phon and 3.52 sone. Compared to the aircraft noise, road traffic noise is rather stationary than aircraft noise, as the aircraft noise is occasional signal with one flyover and road traffic noise sounds continuously with pass-by cars.

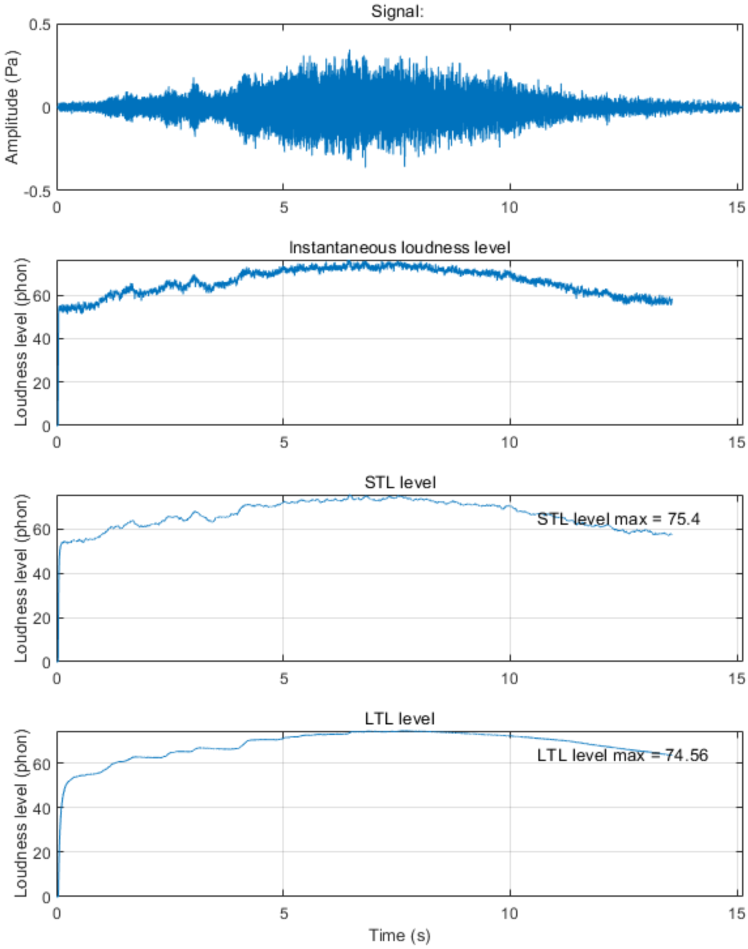

Figure 2.6 Amplitude, Instantaneous loudness level, Short-term loudness level and long-term loudness level of aircraft noise with 68 dB(Left ear) in phon unit

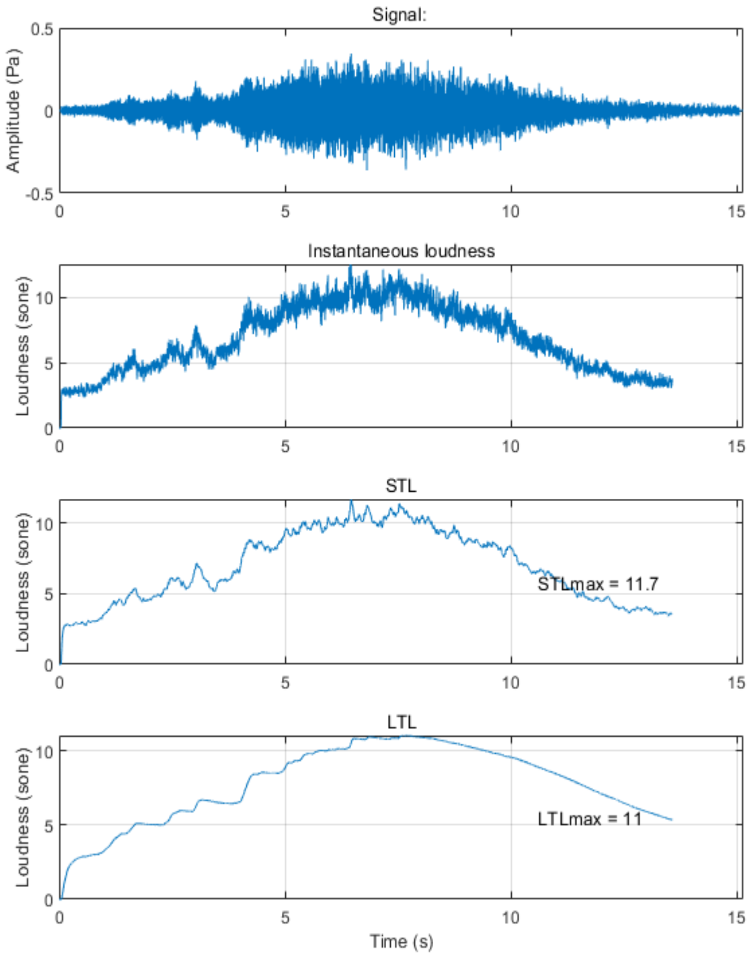

Figure 2.7 Amplitude, Instantaneous loudness level, Short-term loudness level and long-term loudness level of aircraft noise with 68 dB(Left ear) in sone unit

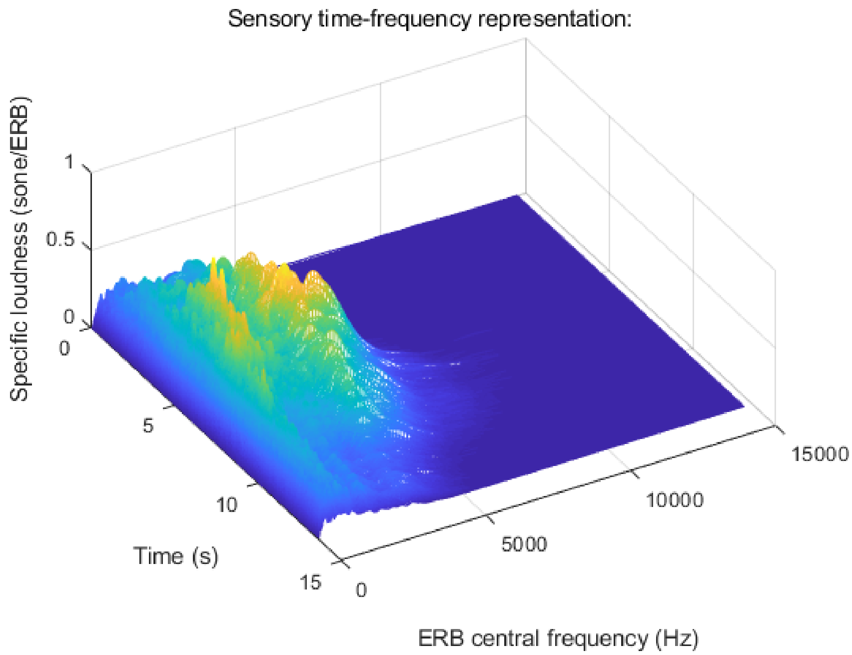

Figure 2.8 Sensory time-frequency representation of aircraft noise with 68dB in left ear

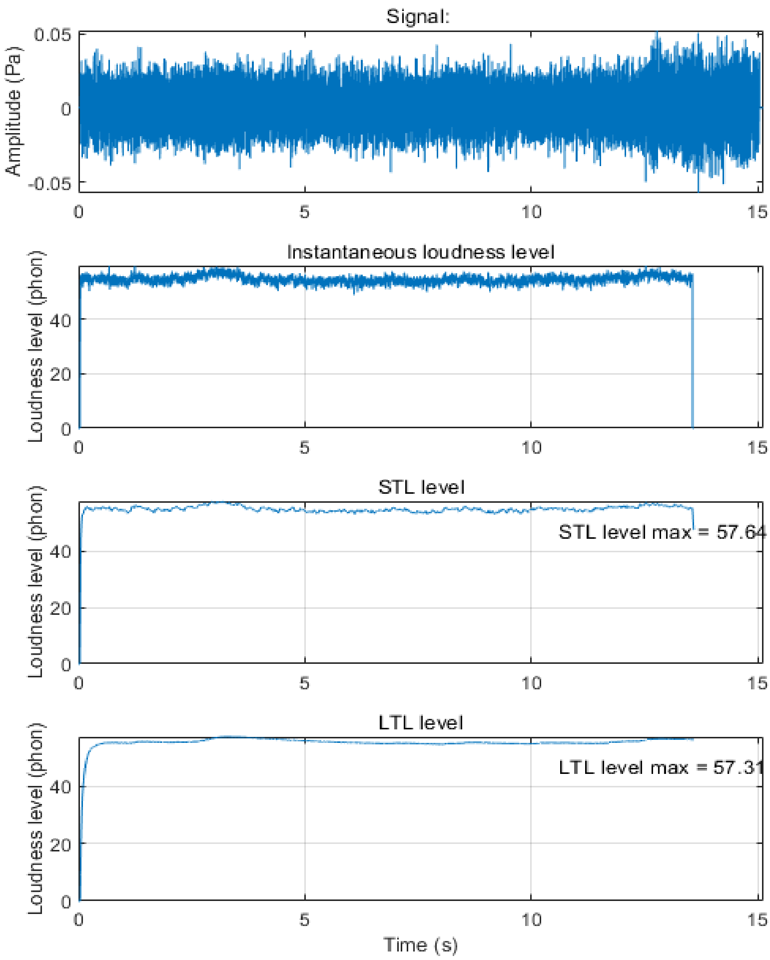

Figure 2.9 Amplitude, Instantaneous loudness level, Short-term loudness level and long-term loudness level of road traffic noise with 55 dB(Left ear) in phon unit

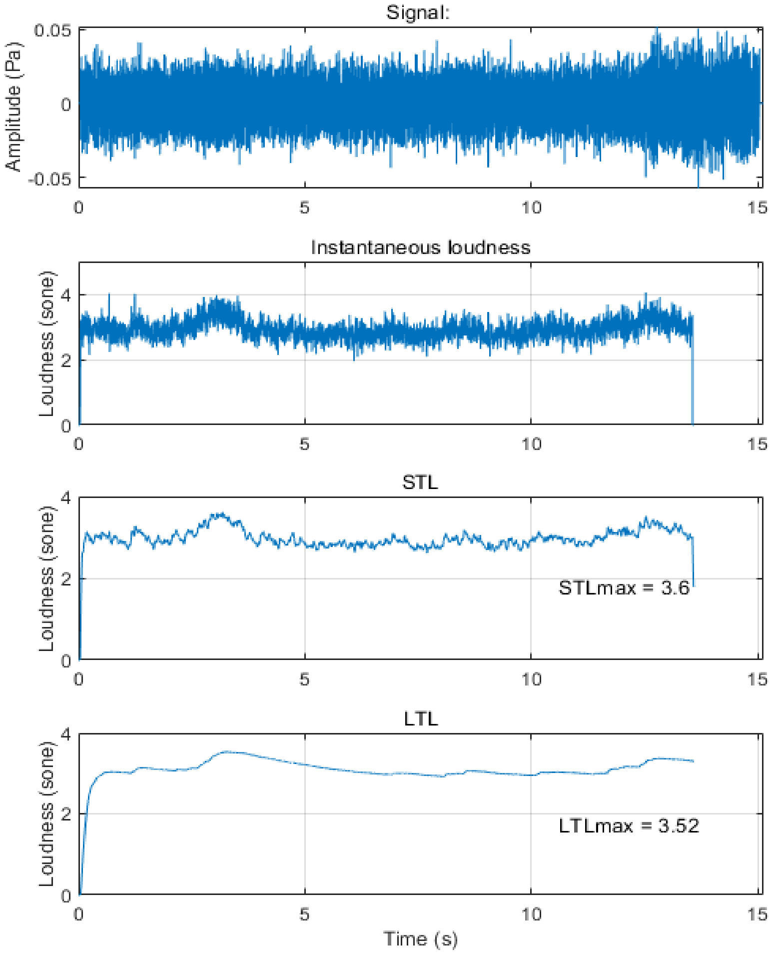

Figure 2.10 Amplitude, Instantaneous loudness level, Short-term loudness level and long-term loudness level of road traffic noise with 55 dB(Left ear) in sone unit

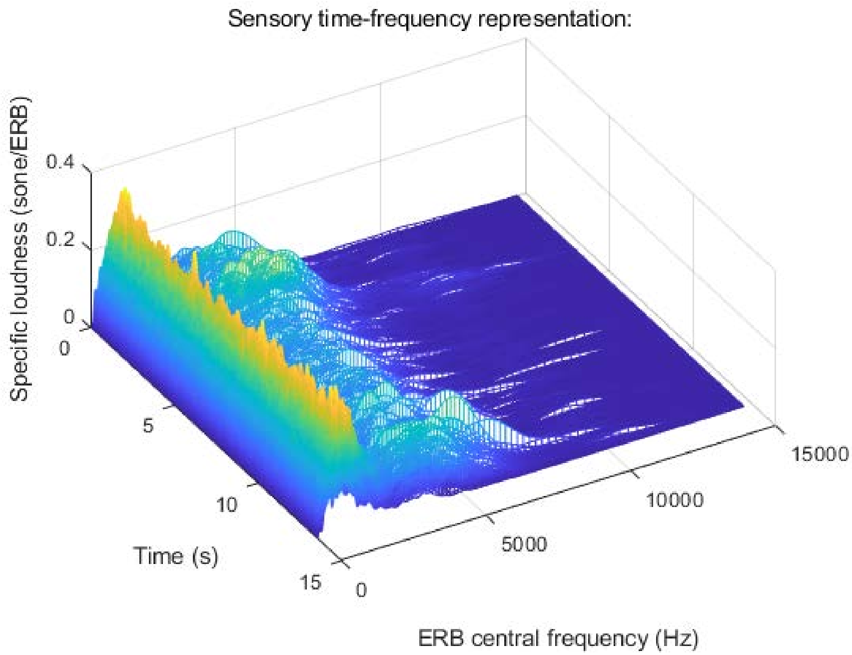

Figure 2.11 Sensory time-frequency representation of road traffic noise with 55dB in left ear

2.4.3 Experimental Equipment

The composition of test equipment is depicted in figure 2.12.

The test is conducted with laptop connected to digital-to-analog converter and signal data acquisition hardware, LAN XI by B&K. DAC executed the sounds from laptop to headphone with flat frequency response (SRH1840) and LAN XI worked for the calibration of output signals to adjust the targeted noise levels. Subjects wear the headphone and follow the instructions that appear in the laptop screen.

2.4.4 Test Procedure

The validation procedure is as follow.

Subjects first listen to the aircraft noise stimuli without the background noise.

Next, subject listen to the aircraft noise stimuli with the road traffic noise as a background sound

Then the pre-programed computer asks if the noise in background is louder, quieter, or same compared to the noise without road traffic noise.

The program adjusts the stimuli with the road traffic noise from the answer of subjects. For example, if the subject selects louder, then the noise level of background sound is lower in the next session. The steps of level change are decreasing from 5dB to 1dB.

The test proceeds until the subject select the “same.”

All the test procedures are pre-programed by MATLAB so that subjects read

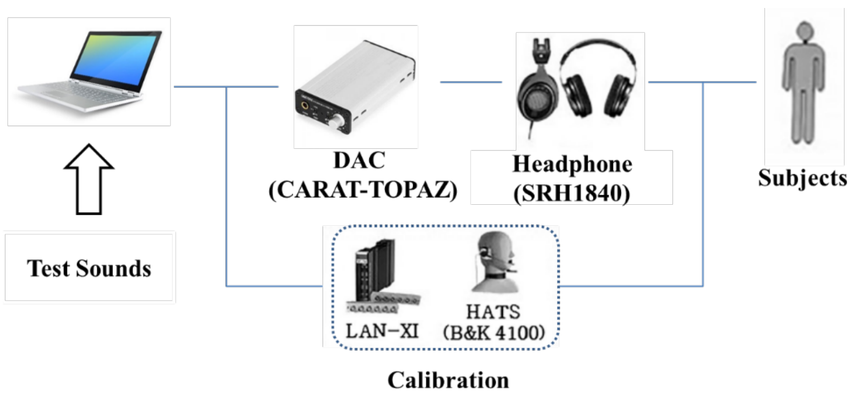

Figure 2.12 Test Equipment for Laboratory Test

the instructions listen to the stimuli and enter the test results without existence of experimenter. The test lasts about 90 minutes with three 5-minute break when the background noise level changes.

2.4.5 Results

The test results are listed in Table 2.1.

In the experimental results, subjects hear the same loudness level if the aircraft noise level in road traffic noise is higher than the sound in quiet. The gap between two noises grow as the background noise levels increase. This background noise effect is shown in former researches.

Next, with the help of partial loudness model with binaural inhibition, partial loudness of each stimulus is calculated. By calculating several levels near the stimuli, equal loudness curves of noise in quiet and with background noise is achieved. These curves and the test results are depicted in same graph to compare the predicted results and the experimental results. The graph with standard deviation is depicted in figure 2.13.

As shown in the above figure, the experimental values follow the predicted curves and this result shows that partial loudness model with binaural inhibition well predicts the loudness of environmental noises. From the validation of the model, all the following calculations of partial loudness by combined noises are now executed with partial loudness model of binaural inhibition which is newly proposed in this study.

Table 2.1 Results of Validation Test for Partial Loudness Model with Binaural Inhibition

Aircraft Noise (dB)	Road Traffic Noise (dB)	Experimental Results (dB)	Predicted Results (dB)	Gap
68	**55**	**68.6**	**69.1**	**0.5**
73		**73.1**	**73.6**	**0.5**
78		**78.3**	**78.3**	**0.0**
68	**65**	**70.2**	**70.9**	**0.7**
73		**74.1**	**74.9**	**0.8**
78		**78.7**	**79.1**	**0.4**
68	**75**	**73.4**	**74.3**	**0.9**
73		**77.4**	**77.4**	**0.0**
78		**80.1**	**80.9**	**0.8**

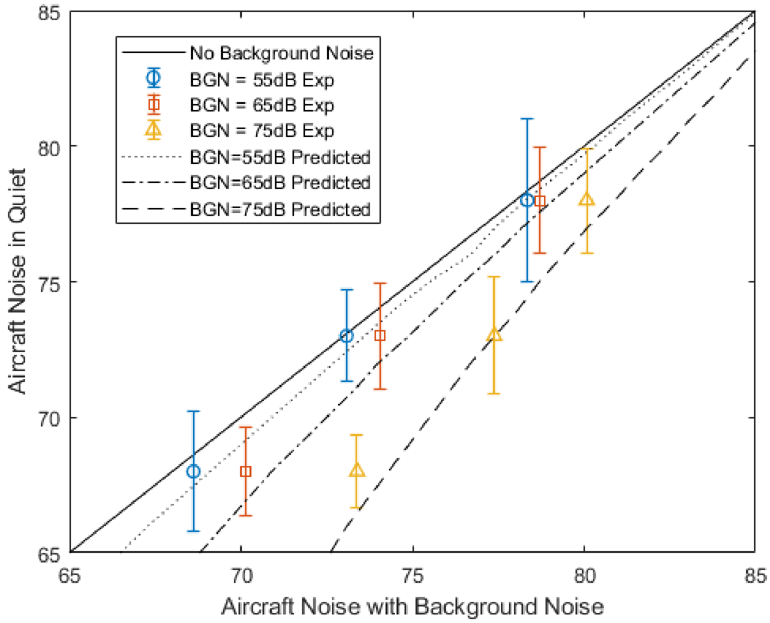

Figure 2.13 Comparison between Experimental Results and Predicted Results

Chapter. 3

Short-term Annoyance Model of Combined Noise from Aircraft and Road Traffic Noise

From the validation of partial loudness model with binaural inhibition, it is capable to calculate the loudness of combined noise regarding background noise and binaural effects. In this section, annoyance model of combined noise from aircraft and road traffic noise in the environment of short-term noise exposure is derived. The laboratory test is conducted to deduce the method of annoyance calculation and partial loudness is the main factor to deduce the combined noise annoyance.

3.1 Laboratory Test

For modeling of short-term annoyance with combined noises, jury test was conducted. The test was proceeded in the same anechoic chamber which validation experiment of partial loudness model was conducted. The test stimuli were selected as same sounds as the validation test used. The experimental equipment that were used in this test were also same as the former test.

Total 44 subjects participated in the experiment with 17 females and 27 males, with an age range of 20–31 (mean 25, standard deviation 3.2). All the participants conducted the screening test for normal hearing and founded out to be normal.

3.2 Stimuli

The stimuli of laboratory test for annoyance evaluation are same as section.2.3.2, while two levels of aircraft and road traffic noises are added. Aircraft noise levels are prepared from 63 to 83 dBA with 5 dBA intervals, and road traffic noise are adjusted from 55 to 75 dBA with also 5 dBA intervals. The unit of noise level is L_{Aeq}.

3.3 Test Procedures

The test procedures are as follow.

The subjects hear the test stimuli and experimenter announced that these sounds will be played for the test.

Subjects hear the aircraft noise in quiet and were asked how annoying the sounds are. They rated the annoyance with 11-length scale with 0 as not annoyed at all and 10 as extremely annoyed.

Subjects hear the road traffic noise in quiet and were asked how annoying these sounds are and they also rated the annoyance with 11-length scale.

The aircraft noise with road traffic noise is played and the subjects were asked how annoying the aircraft noises are in the presence of road traffic noise. They scored the annoyance of aircraft noise in 11-length scale.

The road traffic noise with aircraft noise is played and the experimenter asked the subjects how annoying the road traffic noises are in the existence of aircraft noise. Participants rated the annoyance in 11-length scale.

The combined noise of aircraft and road traffic noise is played, and the subjects were asked how annoying the total combined noises are and they rated the annoyance in 11-length scale.

Total 85 noises, with five aircraft noises, five road traffic noises, twenty-five combination of aircraft noise with road traffic sounds, twenty-five combined noises of road traffic noise with aircraft sounds, and twenty-five aircraft and road traffic noise combination, were played and the test lasts about 70 minutes.

3.4 Results

The test results are listed in Table 3.1 to 3.4. Table 3.1 presents the annoyance results of aircraft and road traffic noise without background sounds. Table 3.2 shows the values of annoyance from aircraft noise with road traffic noise as background noise. Table 3.3 is the results of annoyance from road traffic noise with aircraft noise as ambient sound, and Table 3.4 shows the annoyance of combined noise of aircraft and road traffic noise.

From the test results, the annoyance values show the strong relationship with target noise level as the level of main source increases, the annoyance rating

Table 3.1 Results of annoyance and loudness from aircraft and road traffic noise in quiet

	Aircraft Noise	Road Traffic Noise	Annoyance	Loudness
Aircraft Noise in Quiet	63	-	3.3	8.8
	68		4.4	17.7
	73		5.5	15.5
	78		6.7	20.5
	83		8.0	26.9
Road Traffic Noise in Quiet	-	55	1.1	3.6
		60	2.2	5.1
		65	2.5	7.1
		70	4.3	9.6
		75	5.8	12.9

Table 3.2 Results of annoyance and partial loudness from aircraft noise with road traffic sound as background noise

	Aircraft Noise	Road Traffic Noise	Annoyance	Loudness
Aircraft Noise with Road Traffic Noise	63	55	2.7	7.8
	68		4.0	11.0
	73		4.6	15.0
	78		6.5	20.1
	83		8.2	26.7
	63	60	2.8	6.9
	68		3.8	10.3
	73		4.9	14.5
	78		6.5	19.7
	83		8.0	26.4
	63	65	3.0	5.6
	68		4.0	9.1
	73		5.4	13.5
	78		6.7	19.0
	83		8.0	25.8
	63	70	2.9	4.2
	68		4.5	7.4
	73		5.2	12.0
	78		6.5	17.8
	83		7.7	24.9
	63	75	3.3	2.3
	68		4.6	5.4
	73		5.3	9.7
	78		6.7	15.7
	83		7.9	23.2

Table 3.3 Results of annoyance and partial loudness from road traffic noise with aircraft sound as background noise

	Aircraft Noise	Road Traffic Noise	Annoyance	Loudness
Road Traffic Noise with Aircraft Noise	63	55	1.3	2.1
		60	1.7	3.6
		65	2.5	5.8
		70	3.7	8.5
		75	5.9	12.0
	68	55	1.5	1.5
		60	1.9	2.9
		65	2.3	5.0
		70	4.1	7.8
		75	5.6	11.4
	73	55	1.4	0.8
		60	2.1	2.0
		65	2.8	4.0
		70	3.9	6.7
		75	5.9	10.3
	78	55	1.5	0.4
		60	2.1	1.2
		65	2.2	2.8
		70	3.9	5.4
		75	5.3	9.0
	83	55	2.0	0.2
		60	2.1	0.6
		65	2.8	1.6
		70	3.4	3.7
		75	5.7	7.1

Table 3.4 Results of annoyance and loudness from combined noise of aircraft and road traffic noise

	Aircraft Noise	Road Traffic Noise	Annoyance	Loudness
Aircraft and Road Traffic Noise	63	55	3.1	8.9
	68		3.7	11.8
	73		4.8	15.6
	78		6.7	20.5
	83		7.9	26.9
	63	60	3.3	9.1
	68		4.1	11.9
	73		5.1	15.6
	78		6.0	20.6
	83		7.9	27.0
	63	65	3.5	9.6
	68		4.6	12.2
	73		5.6	15.8
	78		6.1	20.6
	83		8.2	27.0
	63	70	4.5	10.7
	68		5.1	12.9
	73		5.7	16.2
	78		6.9	20.8
	83		8.1	27.1
	63	75	6.0	13.2
	68		6.0	14.2
	73		7.1	17.0
	78		7.1	21.3
	83		8.5	27.4

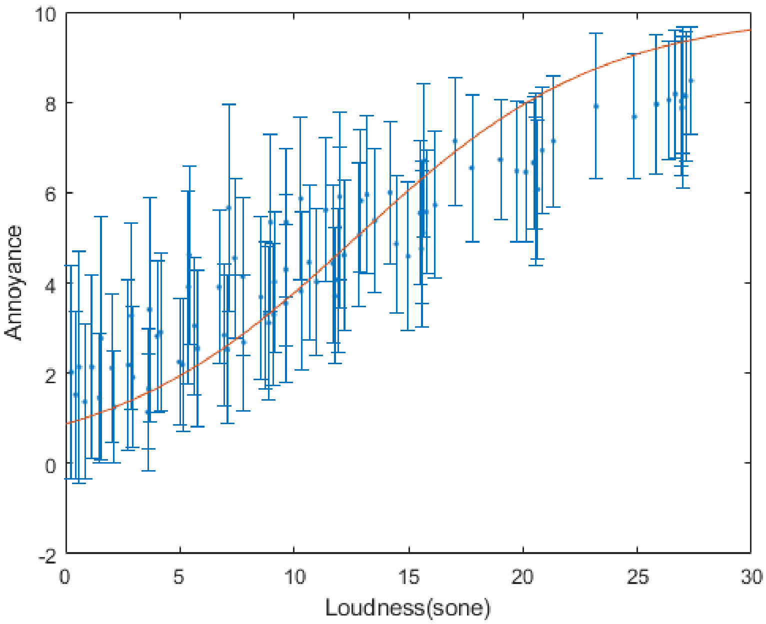

Figure 3.1 Relationship between Loudness and Annoyance of Combined Noise from Aircraft and Road Traffic Noise

also grows. However, the annoyance values of same target noise with different background noise level are appeared with distinction as the level of background noise decreases, the annoyance of target sound increases.

To consider not only the target noise but also the background sound for deriving the annoyance of combined noises, loudness factor, especially partial loudness, is adopted. From the earlier researches, the primary factor that has the strong relationship with perceived annoyance is suggested as loudness [30,31,32]. In this research, loudness is adopted as the independent variable to calculate the dependent variable, annoyance.

After the experiment, single, partial and total loudness of each test sound were calculated with the help of partial loudness model with binaural inhibition. When calculating the partial loudness, aircraft noise is adopted as target sound when the test results are for the annoyance of aircraft noise in the presence of road traffic noise, and vice versa. The calculated loudness values of test stimuli are listed in Table 3.1 to 3.4 with the unit of sone.

As the calculated loudness values are in the same scale, all the results of calculated loudness values are posed in the horizontal axis with each mean annoyance ratings in the vertical axis, as depicted in figure 3.1. From experimental results, a relationship of annoyance-loudness is recognized so that regression between loudness and annoyance rating is conducted.

Former studies executed linear regression, yet as the independent variable increases, dependent variable increases without limit. However, in this study annoyance rating has the limit of 10 so that linear regression is not appropriate to apply. In many regression methods, logistic regression is a statistical model with a form of logistic function as expressed in equation 3.1.

$$\mathrm{f(x)} = \frac{L}{1 + e^{-k(x-x_0)}} \tag{3.1}$$

In the equation, x_0 is the value of sigmoid's midpoint, L is the curve's maximum value and k is the logistic growth rate. The logistic function has the maximum limit so that infinite value of independent variable derives the maximum value.

The statistical analysis is accomplished with SPSS by IBM and the derived model is found in equation 3.2.

$$\text{Annoyance} = \frac{1}{0.1 + 1.048 \times 0.831^{\text{Loudness}}} \tag{3.2}$$

The coefficient of determination is 0.939 so that regression curve highly follows the test results. From the model of short-term annoyance, loudness is the only independent variable so that if the loudness of combined noise is known, the annoyance of it is calculated. Also, partial annoyance of combined noise is capable to be calculated if partial loudness of combined noise is derived by the partial loudness model with binaural inhibition.

As the loudness factor implies intensity characteristics as well as frequency features, this model is improved from the former classical models and dose-response models. In addition, by the application of partial loudness concept, contribution of noise sources comprising combined noise is driven so that different noise sources with same total noise levels have distinct annoyance values as the levels of each noise source of combined noise. Lastly, background noise effect is adopted so that same target noises with different background noise levels show distinct annoyance values.

Chapter. 4

Long-term Annoyance Model of Combined Noise from Aircraft and Road Traffic Noise

Long-term annoyance from the combined noise is evoked by the residents who are exposed to combined noises more than a year. Many researchers studied the annoyance of noise to achieve the long-term effect of exposure with field survey [10]. It is different from short-term noise exposure that long-term exposure is related to the adaptation of noise. People with noise exposure for a long time are immune to the source so that annoyance is different from the short-term noise exposure which evokes the direct annoyance. In this chapter, long-term annoyance model of combined noises from aircraft and road traffic noise is derived by the field survey and partial loudness model with binaural inhibition.

4.1 Research Field

For the modeling of long-term annoyance model, research area should be selected in advance. The qualifications for the research area are exposures to aircraft and road traffic noise at the same time. Also, no other noise sources should exist in the field for evaluating only aircraft and road traffic noise sources. Road traffic noise is common in many cities, while aircraft noise is limited to vicinity of airports. Considering those conditions, Yangcheon-Gu, Seoul, South Korea is selected as research field. It is near Gimpo airport so that aircraft flyover routes pass above the field and has complex road traffic system so that residents in this area are exposed to high road traffic noise levels. In addition, industrial or railway noise do not exist in this research field that interfere the aircraft and road traffic noise. The research field is depicted in figure 4.1. Gimpo airport is placed in the upper left of the figure.

4.2 Noise Mapping

First step for the evaluating annoyance of research area is depicting the noise map for the investigation of noise levels from aircraft and road traffic noise. Noise maps are built with commercial software, CadnaA by Datakustik.

To depict the noise map of aircraft noise, annual flight data from Gimpo airport and flyover routes are input to CadnaA. Flight data includes types of aircraft and numbers of aircraft flight at each flyover route. Flight routes are modeled as figure 4.2.

The research area is modeled by 3D geographical data which include contour lines, buildings and roads. The contour lines and the buildings of research area are shown in figure 4.3 and 4.4. Information of Gimpo airport is listed from Table 4.1 to 4.3, which are position, flight path, and the daily average of aircraft flight numbers. Calculation of aircraft noise in research

Figure 4.1 Research area for long-term noise exposure,

Yangcheon-Gu

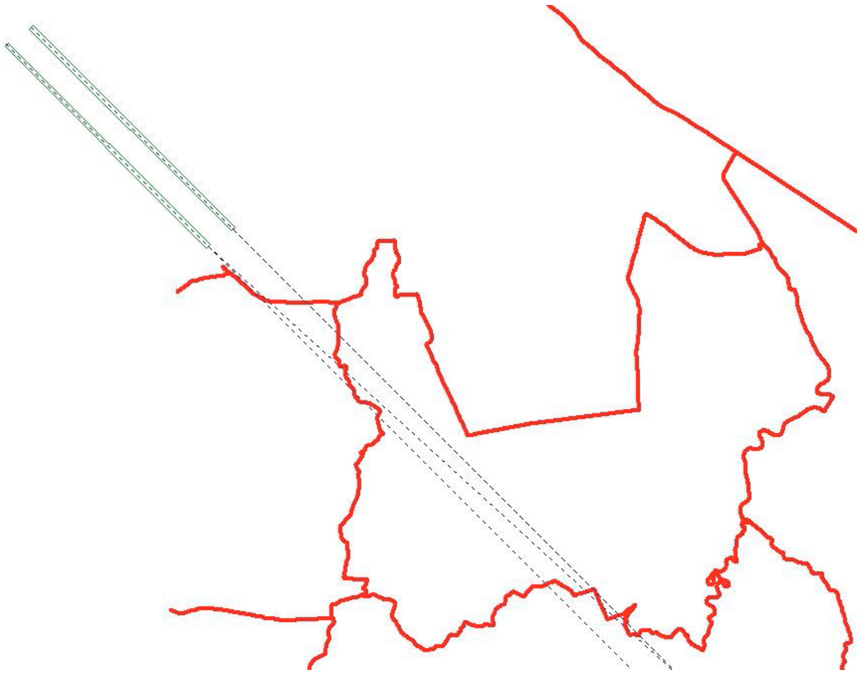

Figure 4.2 Aircraft flight routes of Gimpo airport

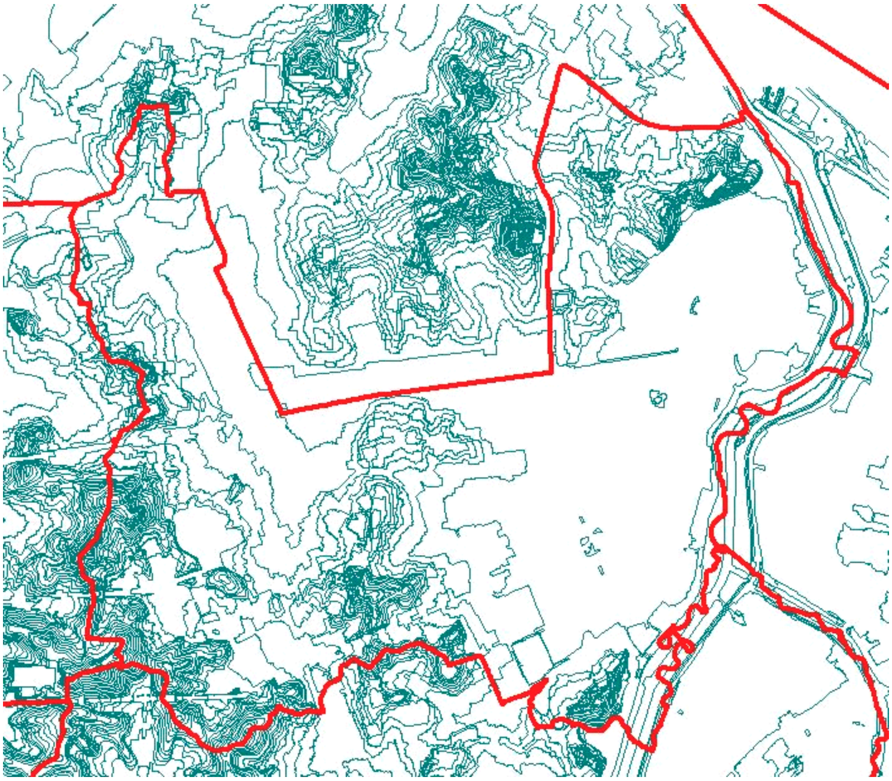

Figure 4.3 Contour lines of research area by CadnaA

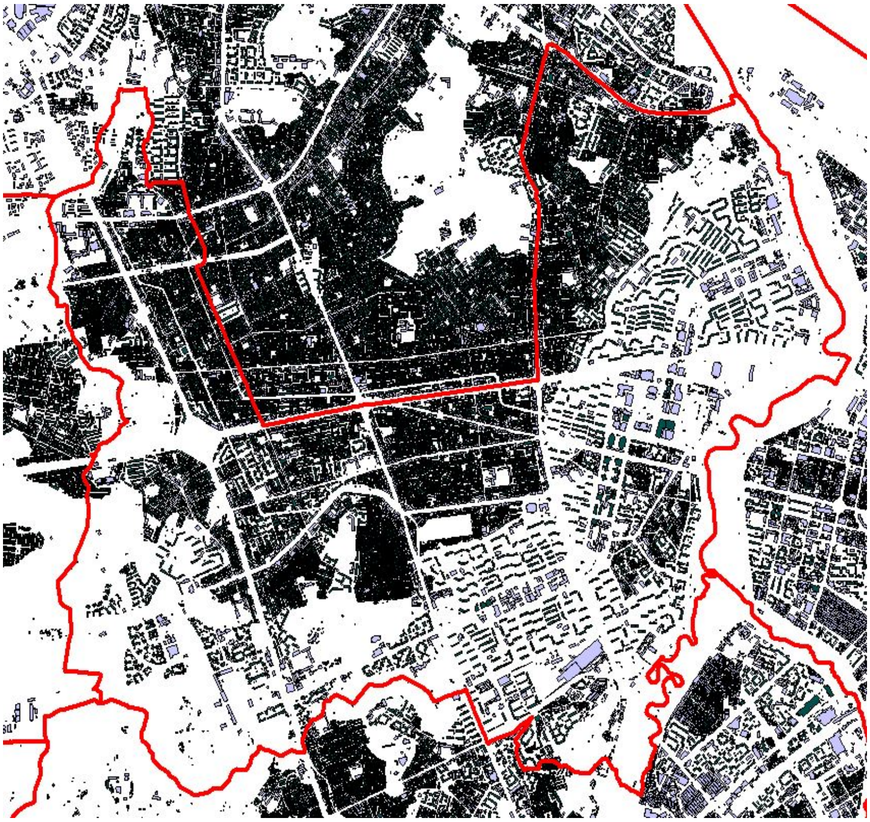

Figure 4.4 Buildings of research area by CadaA

Table 4.1 Position of Gimpo Airport

Runway	Direction(Deg)	Length(m)	Coordinate(WGS84)	
			X	Y
North	135	3480	303850.6	4160441.3
South	135	3480	303552.4	4160229.7

Table 4.2 Flight Path of Gimpo Airport

Runway	Dep/App	Flight Distance(m)	Height(m)	Direction (Deg)
North	Southeast Dep	7408	481.5	135
	Southeast App	10926.8	609.6	135
South	Southeast Dep	7778	481.5	133.4
	Southeast App	10926.8	609.6	135

Table 4.3 Daily Average of Aircraft Flight Number of Gimpo Airport

Aircraft Type	North Runway						South Runway					
	Southeast Dep			Southeast App			Southeast Dep			Southeast App		
	D	E	N	D	E	N	D	E	N	D	E	N
B737	36.2	3.6	1.5	0.2	0	0	0.3	0.1	0	31.2	4.9	1.8
B747	3.5	0.2	0	0	0	0	0	0	0	2.6	0.6	0.2
B757	0	0.2	0	0	0	0	0	0	0	0.1	0.1	0
B767	1.5	0.5	0	0	0	0	0	0	0	1.7	0.2	0.1
B777	0.7	0.2	0	0	0	0	0	0	0	1	0	0
A300	0.1	0	0	0	0	0	0	0	0	0.1	0	0
A320	10.8	1.1	0.6	0	0	0	0.1	0	0	9.4	1.2	0.9
A330	1.6	0	0	0	0	0	0	0	0	0.9	0.2	0.2
MD90	0.1	0	0	0	0	0	0	0	0	0.2	0	0

area is executed by the method of Integrated Noise Model(INM). INM is developed by FAA and is a computer model that evaluate aircraft noise impacts in the vicinity of airports. It uses noise-power-distance(NPD) data to estimate noise accounting for specific operation mode, thrust setting, and source-receiver geometry, acoustic directivity, and other environmental factors. Detail calculating procedures are mentioned in the manual [33]. The noise map from INM are depicted in figure 4.5. The size of the grid is 10m×10m. The unit of aircraft noise is $\mathrm{L}_{A_{eq}}$ which is averaged the annual noise levels of research field. From the noise map, noise levels grow near the airport and flyover routes. Research area has high levels of aircraft noise on the left side while right side has lower levels of it.

To validate the noise map of aircraft, measured data from noise-related institutes were adopted for comparison of measured and predicted levels. The measured points of aircraft noise are plotted in figure 4.6. The results of comparison are listed in Table 4.4 and from the table, aircraft noise map data has good predictability with error extend less than 3dB.

Noise map of road traffic noise is depicted with measured traffic density and noise levels. To predict the road traffic noise of research area, road traffic density, ratio of heavy vehicles, speed limit of each road and materials of roads should be evaluated. The measurement of road traffic density was conducted with three timeslots, with 11:00~11:30, 15:00~15:30 for daytime,

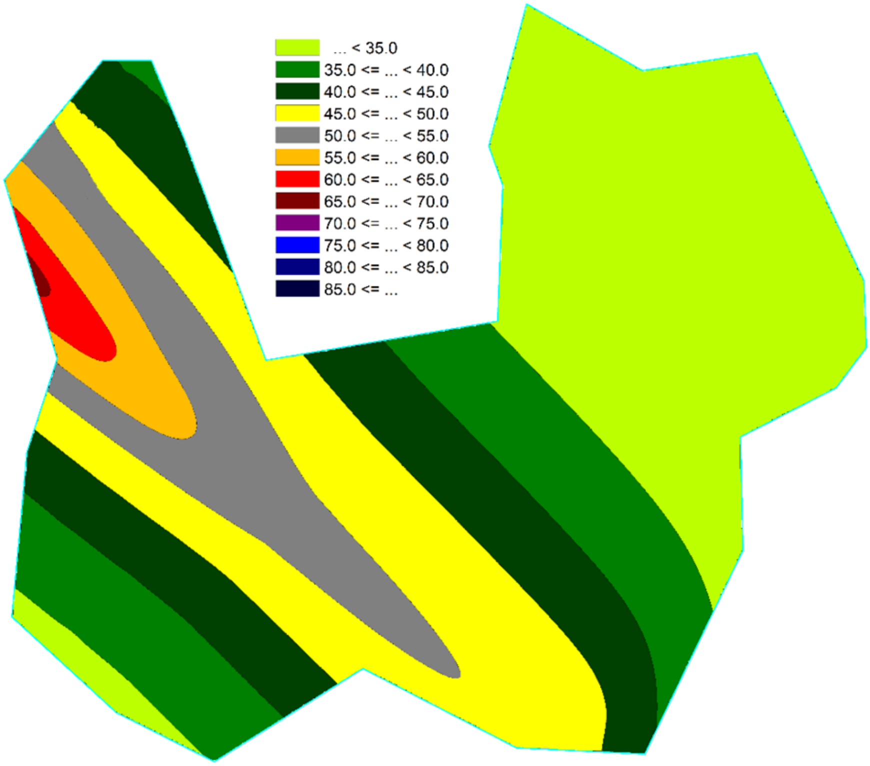

Figure 4.5 Noise Map of Aircraft Noise in Research Area

Figure 4.6 Measuring Points of Aircraft Noise

Table 4.4 Comparison of Measured and Predicted Levels of Aircraft Noise

Points	$L_{A_{eq}}$(dB)		Error
	Measured	Predicted	
A-01	74.4	75.8	-1.4
A-02	82.6	80.7	1.9
A-03	70.5	69.2	1.3
A-04	71.1	71.9	-0.8
A-05	76.3	74.7	1.6
A-06	84.4	81.8	2.6
A-07	76	73.8	2.2
A-08	67.5	68.7	-1.2
A-09	67.2	64.4	2.8
A-10	70.2	71.5	-1.3
A-11	60.4	62.5	-2.1
A-12	79.8	79.2	0.6
A-13	69	68.4	0.6
A-14	79.6	79.4	0.2
A-15	69.7	70.3	-0.6

20:00~20:30 for evening time, 00:00~00:30 and 03:00~03:30 for nighttime. These measuring times were selected to avoid rush hour so that only measure the average traffic density. The 30-minute measured data are doubled for conversion to an-hour-density data and two measured data of one timeslots were averaged. Total 45 points of measurement from intersections of roads were conducted to cover all the roads in research area. Noise levels of road traffic noise were measured in 20 points from wide roads in research field. Measurements were executed at 1.5 meters high from the bottom, as in figure 4.7.

Noise barriers of road traffic were not included in 3D geographical data, so that they were manually added to each road from CadnaA.

Road traffic noise is calculated by CadnaA with the following equations.

$$L_{m,E} = 37.3 + 10\log_{10}[Q(1 + 0.082P)] \tag{4.1}$$

$$L_m = L_{m,E}^{(25)} + R_{SL} + R_{RS} + R_{RF} + R_E + R_{DA} + R_{GA} + R_{TB} \tag{4.2}$$

$$L_m = 10\log_{10}[10^{0.1L_{m,n}} + 10^{0.1L_{m,f}}] \tag{4.3}$$

$$L_r = L_m + K \tag{4.4}$$

The coefficients of road traffic noise model are as follows.

1) $L_{m,E}$: sound emission level at 25m distance from the source under idealized condition (speed 100 (80) km/h for a light (heavy) vehicle, road gradient < 5%, smooth

Figure 4.7 Road Traffic Noise Measurement of Research Area

asphalt)

2) L_m: mean emission level for each lane at a receiver position

3) L_r: Sound level at a receiver position

4) Q : Traffic volume per hour

5) P : Percentage of heavy trucks P (Weight>2.8 tons)

6) K ; Increased effect of light controlled intersections

7) R_{SL} : Correction for the speed limit

7-1) $R_{SL} = L_{Pkw} - 37.3 + 10\log_{10}(\frac{100+(10^{0.1D}-1)P}{100+8.23P})$

7-2) $L_{Pkw} = 27.7 + 10\log_{10}[1 + (0.02v_{Pkw})^3]$

7-3) $L_{Lkw} = 23.1 + 12.5\log_{10}(v_{Pkw})$

7-4) $D = L_{Lkw} - L_{Pkw}$

8) R_{RS} : Correction for road surface (range from 0 to 6 dB for a surface type in terms of a vehicle speed)

8.1) $R_{RS} = 0.6|g| - 3$ for $|g| > 5\%$

8.2) $R_{RS} = 0$ for $|g| \leq 5\%$

9) R_{RF} : Correction for rise and falls along the street

10) R_E : Correction for the absorption characteristics of building surfaces

11) R_{DA} : Attenuation coefficient for the distance and air absorption

12) R_{GA} : Attenuation coefficient due to ground and atmospheric conditions

13) R_{TB} : Attenuation coefficient due to topography and buildings dimensions

In the equations, v_{Pkw} means speed limit ranged from 30 to 130 km/h for light vehicles and v_{Lkw} represents speed limit from 30 to 80 km/h for heavy vehicles. From the measured road traffic density and other data, noise map of road traffic noise is depicted as figure 4.8 with the unit of Laeq and the grid size is 10m×10m. As from the figure, noise levels are high near the roads, especially the wide and high traffic density.

To validate the noise map of road traffic noise, predicted levels from noise map and measured noise levels were compared. 20 measuring points are shown in figure 4.9 and the measurement was conducted by B&K 2250 which is described in table 4.5 and figure 4.10. The results of measured and predicted comparison are listed in Table 4.6. From the table, noise map of road traffic noise has high predictability with error extend less than 2dB.

4.3 Field Survey

The next step is to survey the annoyance data of research area. To select the survey subjects, previously depicted noise maps were applied. From the range of noise levels from aircraft and road traffic noises, total 1,000

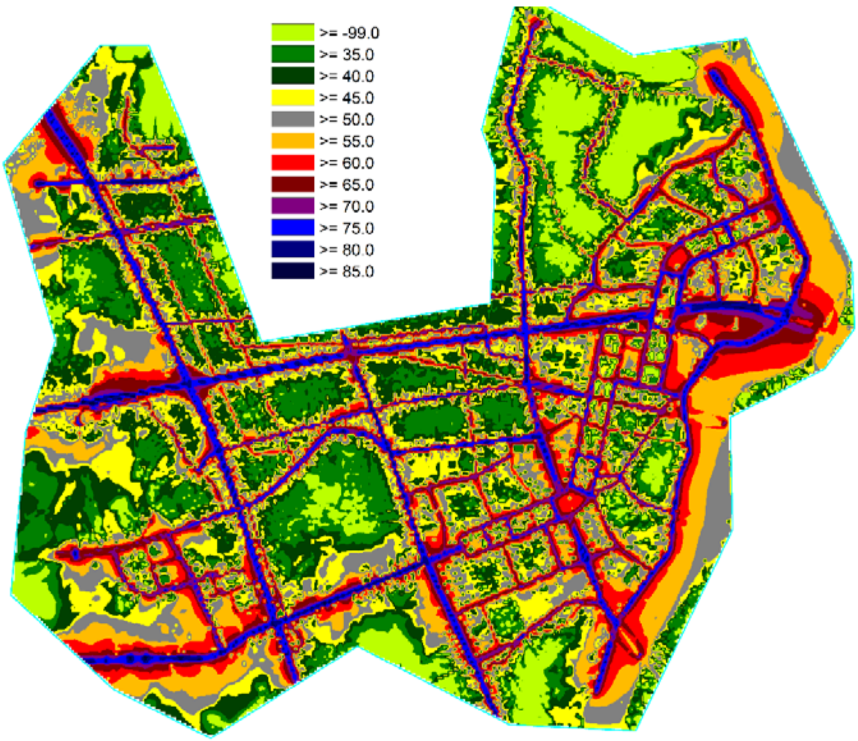

Figure 4.8 Road traffic noise map for research area

Figure 4.9 Measuring points of road traffic noise in research area

Table 4.5 Description of noise measurement equipment

Model	Manufacturer	Description
Type 2250	B&K(Denmark)	Handheld Analyzer (SLM/Frequency Analysis/Logging Software)

Figure 4.10 B&K 2250

Table 4.6 Comparison of measured and predicted levels of road traffic noise

Points	Measured	Predicted	Error
R-01	77.4	76.4	1.0
R-02	79.5	78.5	1.0
R-03	78.9	78.2	0.7
R-04	68.9	70.3	-1.4
R-05	75.9	75.7	0.2
R-06	74.1	76.0	-1.9
R-07	74.6	73.9	0.7
R-08	77.7	77.3	0.4
R-09	75.0	76.5	-1.5
R-10	71.7	71.8	-0.1
R-11	75.9	74.1	1.8
R-12	72.5	73.4	-0.9
R-13	74.3	74.4	-0.1
R-14	74.5	73.8	0.7
R-15	72.8	71.8	1.0
R-16	79.5	78.9	0.6
R-17	83.9	83.4	0.5
R-18	68.7	68.3	0.4
R-19	77.3	76.5	0.8
R-20	75.9	75.3	0.6

subjects were selected with their noise exposed standards. Highly exposed population by aircraft noise is small as a few of residences near the Gimpo airport exists. The selected scope of noise levels and the numbers of subjects are listed in table 4.7 and table 4.8 shows the social demographical data of the subjects.

The survey was conducted by visiting the residence of subjects and ask if they are feasible to participate in the investigation of aircraft and road traffic noise annoyance. Researchers inquire the annoyance of aircraft noise in the presence of road traffic noise to the subjects when they rest in home, and vice versa. The subjects answer their annoyance ratings in 11-length scale with 0 as not annoyed at all and 10 as extremely annoyed.

For connection between noise map information and self-reported survey data, earlier study revealed that self-report of noise exposure and noise map information are consistently associated when the aircraft noise is considered [34]. Also, in other research, the correlation between noise annoyance and noise exposure levels of road traffic noise is fair [35]. Therefore, in this research, social survey data regarding annoyance ratings and the noise levels from noise maps of aircraft and road traffic noise are analyzed for the derivation of the model for the combined noise annoyance.

4.4 Results

The partial loudness values of aircraft and road traffic noise with binaural inhibition in each residence of the subject are calculated by the model of partial loudness. Total 1,000 partial loudness values are deduced regarding the type of background noise. In long-term annoyance, value of %HA, which is called percentage of highly annoyed, is adopted. This factor represents the percentage of residents who score the annoyance rating more than 8 in 11-length scale. To calculate the percentage, the values of loudness are grouped in certain ranges. In this study, 9 groups are generated with the range of loudness in 5 sone. With the values of partial loudness and %HA, a relationship between them is drawn as same as done with the short-term annoyance model, and depicted in figure 4.11

As with the same method applied in modeling the short-term annoyance, logistic regression between partial loudness and %HA is adopted to model the long-term combined noise annoyance of aircraft and road traffic noise. The deduced equation is expressed in equation 4.5.

$$\%\mathrm{HA} = \frac{1}{0.01 + 0.043 \times 0.97^{\mathrm{Loudness}}} \qquad (4.5)$$

The coefficient of determination is 0.882, which is that regression curve follows the survey results well. Equation 4.5 is the final form of long-term annoyance model of combined noise from aircraft and road traffic noise. If the noise levels of aircraft and road traffic noise from research field are known, the percentage of highly annoyed residents are deduced from the model.

Comparing the newly developed model to former annoyance model which is Miedema's model is depicted in figure 4.12. As the model of Miedema adopted equivalent noise level of aircraft and road traffic noise, conversion to total loudness of subjects' noise levels is necessary for the comparison of two models. In the figure, the tendency between loudness and annoyance is similar, while the suggesting model in this research has the higher annoyance value. It can be explained as the newly developed model includes not only the total annoyance of combined noise, but also the partial annoyance of aircraft and road traffic noise. Also, annoyance is subjective value from psychoacoustics so that distinctions occur from countries, regions and even subject themselves. From the result of comparison, it is suggested that the newly developed model of annoyance from combined noise is more adequate to subjects who live in South Korea, while the former model is suitable for the residents in Europe.

The newly developed model of long-term annoyance is later adopted to draw the annoyance map of combined noise from aircraft and road traffic noise.

Table 4.7 Scope of noise levels and number of subjects

Aircraft Noise	Road Traffic Noise	Subjects
Over 83dB	Over 70dB	62
78~83dB	60~70dB	210
73~78dB	50~60dB	274
Less than 73dB	Less than 50dB	454
Total		1000

Table 4.8 Social Demographical data of survey subjects

Contents		Less than 55dB	55-65dB	Over 65dB	p-value
Age		45.4± 16.8	44.6± 16.1	46.9± 15.6	0.398
Residential Period(year)		8.5± 8.4	7.9± 7.3	7.0± 5.9	0.112
BMI		23.8± 3.7	23.9± 3.7	22.7± 3.2	0.405
Sex	**Male**	266	123	59	0.534
	Female	314	152	86	
Educational level	**Secondary Level**	239	94	52	0.092
	University Level	335	181	91	
Marriage	**No**	205	100	44	0.462
	Yes	372	175	100	
Monthly income(1,000 Won)	**<3,000**	309	126	53	<0.001
	⩾3,000	211	133	81	
Smoking	**No**	469	250	126	0.001
	Yes	111	25	19	
Drinking	**No**	314	173	90	0.027
	Yes	266	102	55	
Exercise	**No**	417	183	101	0.277
	Yes	163	92	44	

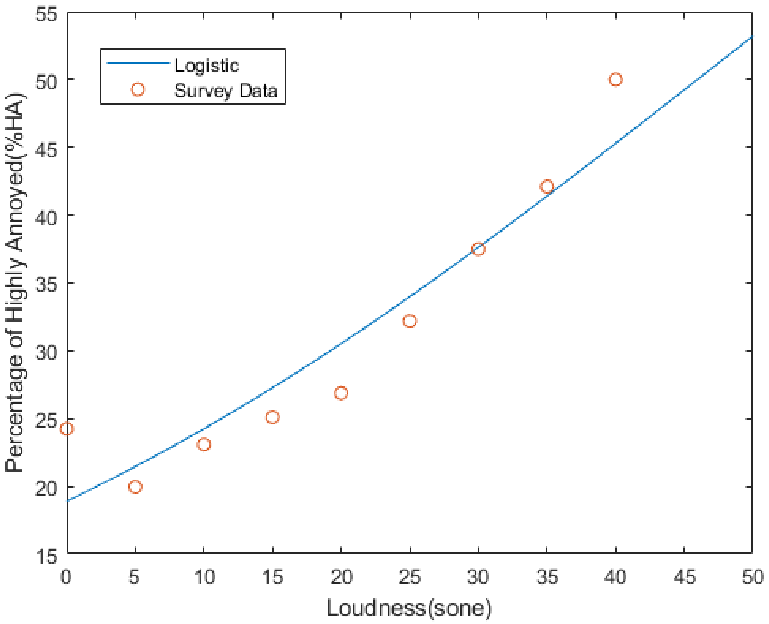

Figure 4.11 Regression between loudness and %HA of long-term noise exposure to combined noise from aircraft and road traffic noise

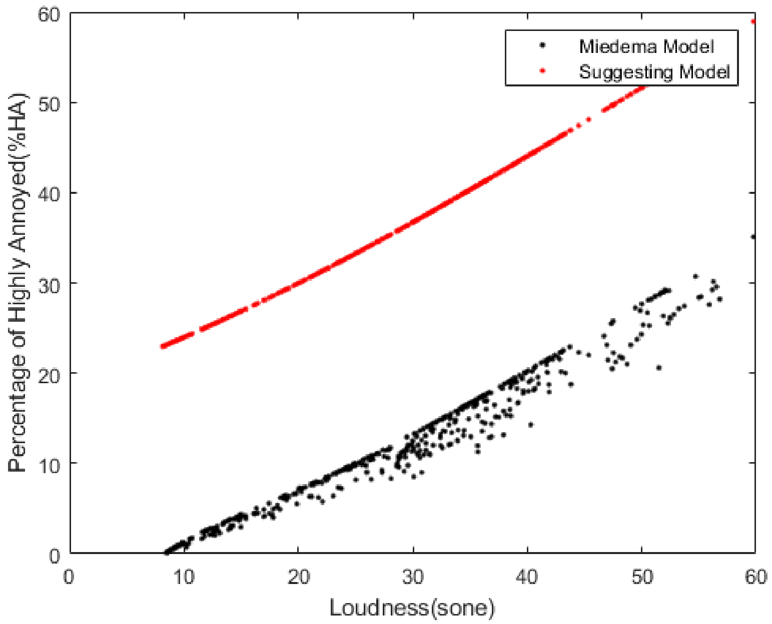

Figure 4.12 Comparison between newly suggested model in this study and Miedema's annoyance model

Chapter. 5

Annoyance Mapping

With the help of the long-term annoyance model of combined noises from aircraft and road traffic noise, annoyance maps that presents the annoyance of combined noises regarding research field are drawn. Distinct from former noise maps, annoyance map shows how residents of noise exposure feel about the sounds of aircraft and road traffic noise, as well as partial annoyance considering background noise effect. In this chapter, procedures of annoyance mapping is described in detail.

5.1 Literature Reviews

Annoyance map was first suggested by Knauss, for the purpose of visualization of annoyance on noise exposure [36]. With the application of 'Response function for environmental noise in residential areas' [37], the annoyance potentials are derived by the noise levels depending on the source types. The combined annoyance is calculated as equation 5.1.

$$P_n^{CA} = \sum_{j=1}^{n}(1 - \sum_{k=1}^{j-1} P_k) \cdot P_j \qquad (5.1)$$

In the equation, P_n^{CA} is the combined annoyance of n noise sources and P_j represents the annoyance for source j in %/100.

By the equation, the annoyance map of combined noise can be depicted. However, it only shows the total annoyance from each noise sources so that partial annoyance which includes the contribution on annoyance for each source is not considered. Also, Annoyance values are derived by the physical values which is noise levels, yet as the annoyance is a psychoacoustical factor, values of same category shows higher relationship with it.

In other research, annoyance map by road traffic noise is drawn with the survey data and analysis of percentage of highly annoyed [38]. However, in this study, only single noise source is considered and depict the annoyance map only from the survey data, not by the noise levels.

In this chapter, advanced annoyance mapping procedures are suggested in consideration of source contribution and high correlation with annoyance factor.

5.2 Annoyance Mapping Procedures

5.2.1 Extraction of grids from noise maps

The first step is to extract the grids of noise map to collect the physical noise levels of research fields. In chapter 4, noise maps of aircraft and road traffic noise were depicted in research field. The extraction is executed by noise mapping program, CadnaA. Noise maps present noise levels from the sources by each grid which the users defined. In this research, the grid size is defined as 10m×10m. Total 716,975 grids were extracted with each noise map, and each grid contains noise levels of aircraft and road traffic.

5.2.2 Calculation of partial loudness and annoyance

By adoption of long-term annoyance model, the partial loudness of each grid are calculated. The partial loudness values are deduced in two cases, with the loudness of aircraft in the existence of road traffic noise, and vice versa. All the loudness values have unit in sone.

The calculated loudness values are converted to %HA by applying the long-term annoyance model in equation 4.5. It results in the representation of the percentage of how annoyed residents would live in.

From the extracted grids at section 5.1.1, the noise level values are converted to %HA, which is essential for the annoyance mapping. From now the grids contain coordinates of each grid and %HA for that position.

5.2.3 Insertion of modified grids to noise mapping program

The modified grids conducted in section 5.2.2 are inserted to CadnaA for the presentation of annoyance, especially %HA, with research field. The steps for extraction and insertion is made as the noise mapping programs including CadnaA have no module or method to calculate loudness and annoyance in themselves. For this reason, loudness and annoyance are calculated out from the program and only the calculated data are inserted to show the annoyance distribution. When the module of calculation for long-term loudness and annoyance of combined noises are added, section 5.2.1 and section 5.2.2 will be deleted and procedures for annoyance mapping will be simplified. The whole procedures are depicted as block diagram in figure 5.1.

5.2.4 Results

The annoyance maps of combined noise regarding aircraft and road traffic noises with binaural inhibition are depicted in figure 5.2 and 53. Figure 5.2 is the annoyance map of aircraft noise from combined noise with road traffic sound as a background noise, and figure 5.3 shows the annoyance map of road traffic noise with aircraft noise as an ambient sound.

As seen from the figure 5.2, it shows highly annoyed distribution in airports, aircraft flyover routes and its vicinity. The map shows that more than half of the residents are highly annoyed by the aircraft noise in these regions. The noticeable point in this map is that annoyance near the roads is shown with less percentages comparing to other fields. It is due to the background noise effect that same noise levels with higher background noise levels have

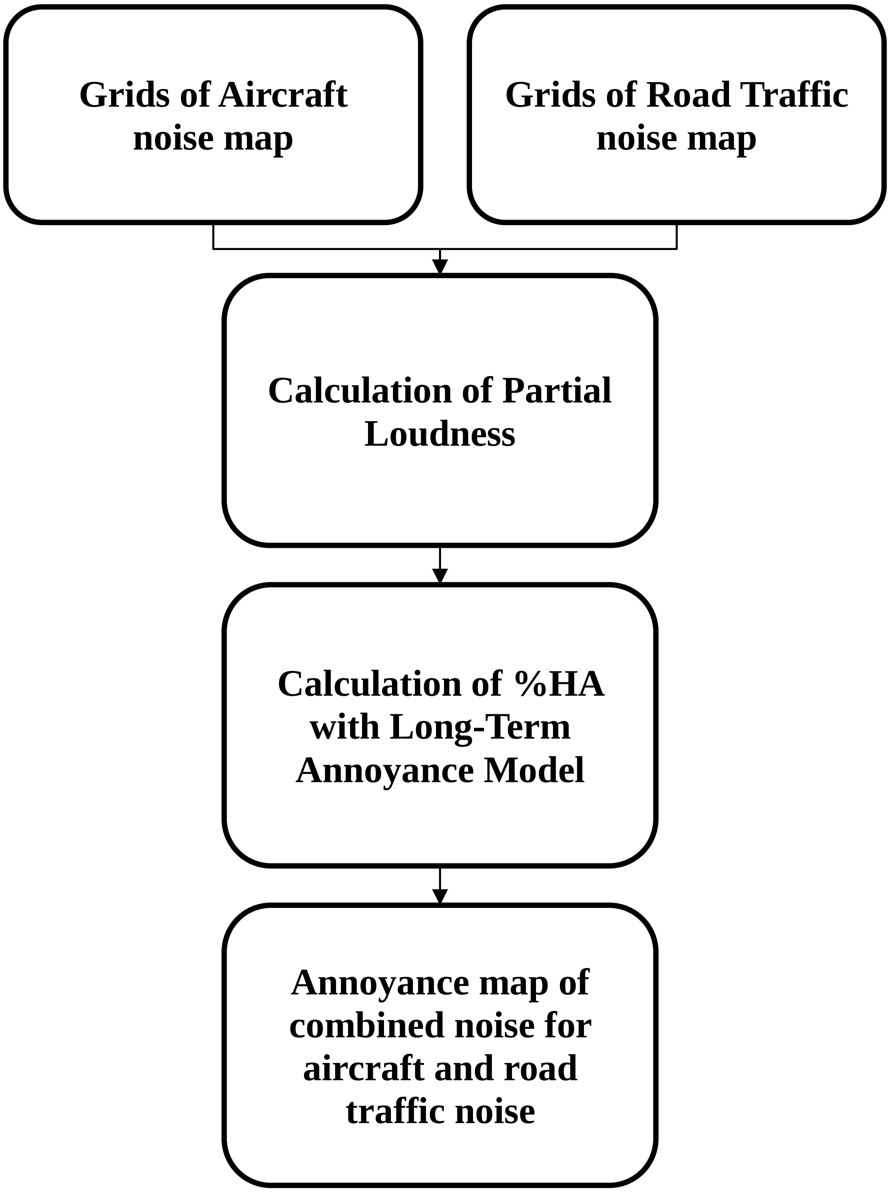

Figure 5.1 Annoyance Mapping Procedures

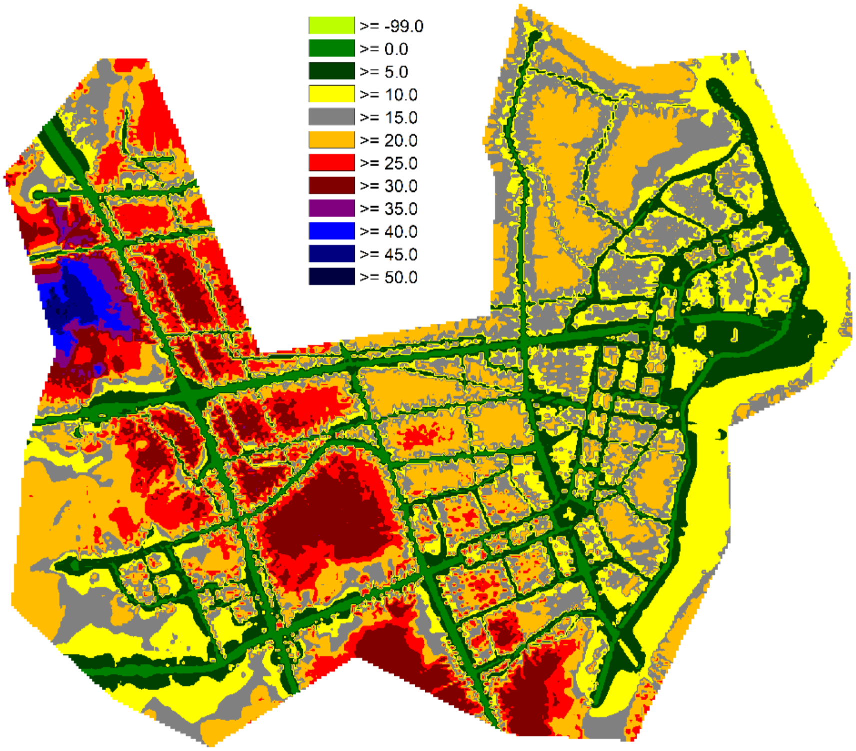

Figure 5.2 Annoyance map of aircraft noise with road traffic noise as background sound

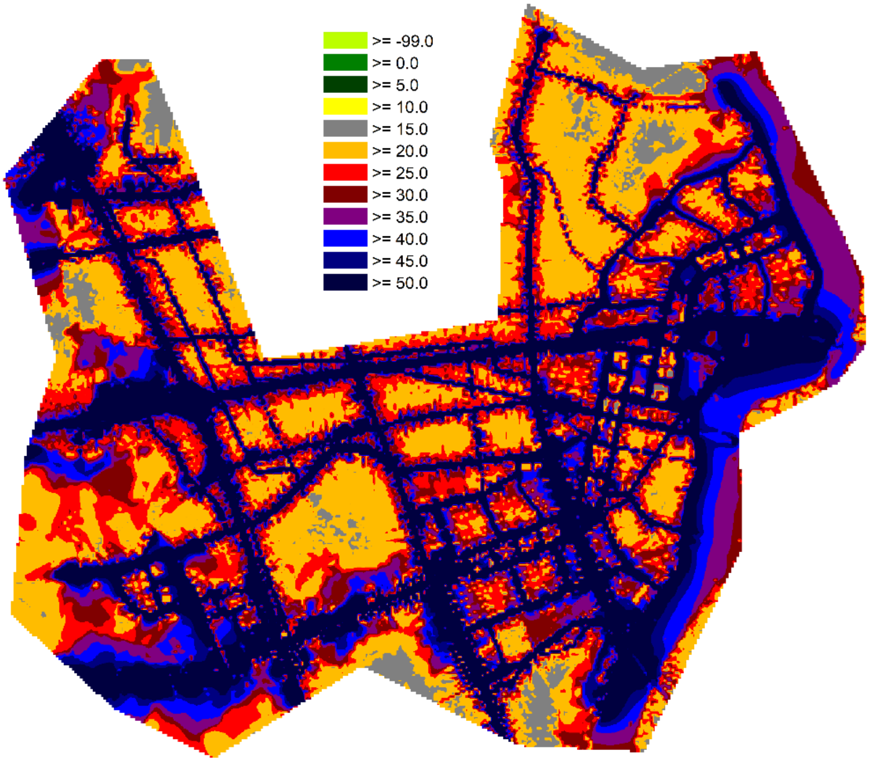

Figure 5.3 Annoyance map of road traffic noise with aircraft noise as background sound

less annoyance values than that with low ambient sound levels [39]. It has not been shown in former noise maps, but the annoyance map first presents this effect.

In figure 5.3, annoyance distributions of road traffic noise are shown with the background noise of aircraft sounds. As similar as the annoyance map of aircraft noise, the map of annoyance from the road traffic noise presents the regions near the source of road traffic noises have higher annoyance than other fields. However, distinct from figure 5.2, the annoyance of road traffic noise shows little effect of background noise as the annoyance near the aircraft routes show no difference from other regions.

As for the differences of background noise effect with aircraft and road traffic noise, two main reasons have the possibility to explain this phenomenon. First, the exposure time and intensity are different between aircraft and road traffic noise. Aircraft noise plays a role as impact noise, while road traffic noise as continuous noise. This distinction affects the different background noise effect with each noise source. For example, road traffic noise as background sound is affect aircraft noise when aircrafts fly over the regions of subjects. However, aircraft noise as ambient sound partially affect the road traffic noise only when the time of aircraft flight moment. Therefore, noise exposure subjects tend to recognize the road traffic noise as background sound, yet it is hardly noticeable of aircraft noise as ambient sound, so that they answer the annoyance rating without consideration of aircraft noise.

Second reason is the difference in physical aspect. By the analysis of long-term partial loudness of aircraft with road traffic noise and road traffic noise with aircraft noise are shown in figure 5.4 and 5.5.

In figure 5.4, it shows the partial loudness of aircraft noise with 63 dB in the existence of road traffic noise with 75dB. Although the level of road traffic noise is higher than the aircraft noise, it is still hearable to recognize the aircraft noise in road traffic noise. Compare to figure 5.4, road traffic noise with aircraft noise is shown in figure 5.5 and it is presented with totally different with former graphs. It shows the partial loudness of road traffic noise with 55dB in the existence of aircraft noise with 83dB. In the graph, the partial loudness is only hearable at the first and the end of road traffic noise playtime. The middle part of it is totally masked by aircraft noise and subjects do not recognize the road traffic noise so that they answer the annoyance rating only with first and end part of test stimuli. These two reasons cause the differences in noise map and annoyance map with aircraft and road traffic noise.

From annoyance maps, the practical reactions to combined noises by the residents are depicted and the background noise effect is shown as the former noise maps could not.

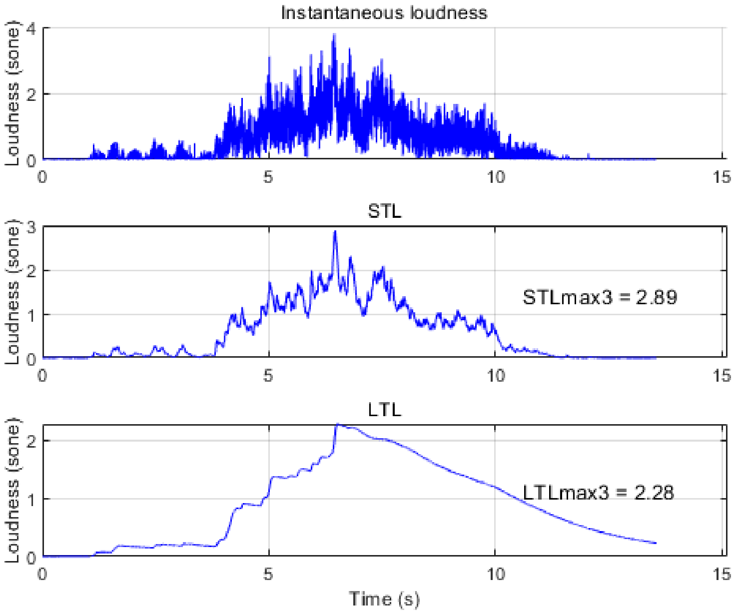

Figure 5.4 Instantaneous, short-term and long-term partial loudness of aircraft noise with 63dB in the existence of road traffic noise with 75dB

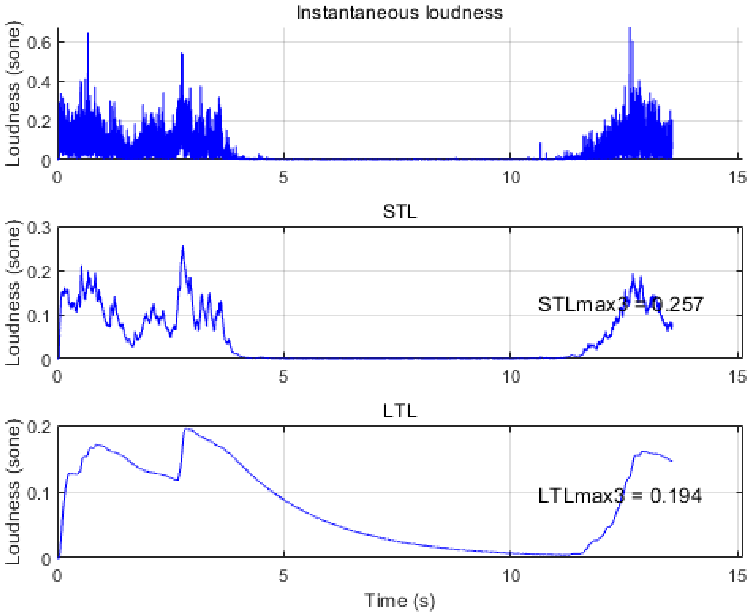

Figure 5.5 Instantaneous, short-term and long-term partial loudness of road traffic noise with 55dB in the existence of aircraft noise with 83dB

Chapter. 6

Conclusions

6.1 Research Summary

By combining the former partial loudness model and loudness model of binaural inhibition, a new model for calculation of partial loudness incorporating binaural inhibition is suggested and validated with laboratory test. Magnitude estimation and adaptive procedure are adapted to the experiment and from the results, the estimated partial loudness with aircraft and road traffic noise incorporating binaural inhibition nearly match with the experimental values.

With the application of partial loudness model with binaural inhibition, a short-term annoyance model for combined noise from aircraft and road traffic noise is developed. A laboratory test was conducted to evaluate the annoyance of aircraft, road traffic and their combined noises. Unlike former studies, not only the total annoyance from single and combined noises of aircraft and road traffic noise are assessed, but also the partial annoyance values from target noise with background sound are evaluated. According to the strong relationship between loudness and annoyance, partial and total loudness from aircraft and road traffic noise are calculated with partial loudness model incorporating binaural inhibition and by the logistic regression, a short-term loudness model for combined noise from aircraft and road traffic noise is developed.

Long-term annoyance model for the combined noise is developed from the field survey and noise mapping. From noise maps of aircraft and road traffic noise from the research area, noise levels are acquired, and subjects of field survey are selected according to their noise exposure levels. Single, partial and total annoyance ratings are evaluated and calculation of loudness values for residences of survey subjects are conducted. With the relationship between loudness and annoyance, long-term annoyance model for combined noises from aircraft and road traffic noises are developed.

Implementing the long-term annoyance model to the noise mapping program deduces the annoyance map of research area. The annoyance maps show how people are annoyed by the combined noises, as well as the single noise source with regard to the background noise. In this research, annoyance map of aircraft noise with background noise as road traffic noise and that of road traffic noise with ambient sound of road traffic noise are depicted. Annoyance maps show the background noise effect as the former noise maps could not. Also, it is shown that how aircraft and road traffic noises act as background noise. In aircraft noise annoyance map, the effect of road traffic noise is noticeable while in road traffic annoyance map, the aircraft noise barely affects the road traffic noise.

6.2 Significances of research

In this research, a new model of partial loudness with binaural inhibition is suggested. As the earlier loudness models only treated the binaural effect as doubling the one-sided loudness values, more accurate method for the loudness of human ear is developed. Loudness itself is the psychoacoustical value so that reactions from human ears must be considered and with the newly suggested model, from now on a binaural loudness from single noises as well as combined noise are able to be calculated.

Short-term annoyance model of combined noises derives the annoyance from sounds played in laboratory environment. With the help of this model, short-term noise exposures from aircraft and road traffic noises can be evaluated without further laboratory tests.

Long-term annoyance model of aircraft and road traffic noise offers the single, partial and total annoyance values from combined noises. If one knows the noise sources at concerning area, the annoyance of that region is directly deduced by the calculation of partial and total loudness factors. It reduces the burden for the wide range of field survey and measuring efforts. Annoyance maps from aircraft and road traffic noise are able to be adopted for the establishment of noise regulations. Former legislations regarding combined noises only considered the total noise levels, not each level of noise source. From now on, by adopting the annoyance map of combined noises, noise contribution of each noise sources consisting the combined noise is revealed so that regulations for the combined noise should change with the consideration of noise source contributions. Also, noise legislations should consider the actual responses from noise, not from the physical levels. As the annoyance map show how residents are annoyed by the combined noises, it can be selected for the evidence to regulate the combined noise by evaluating the highly annoyed regions from the annoyance map.

References

[1] U.S. EPA (U.S. Environmental Protection Agency), Information on Levels of Environmental Noise Requisite to Protect Public Health and Welfare with an Adequate Margin of Safety, 1974

[2] SUTER, Alice H. Standards and regulations. Suter AH ed, 1998

[3] SCHULTE-FORTKAMP, Brigitte, et al. Literaturstudie zur Gesamtgeräuschbewertung. Carl von Ossietzky-Universität Oldenburg, 1996.

[4] BERGLUND, B., & LINDVALL, T., Community noise. Environmental health criteria document. In External review draft. Stockholm: S.U.a.K. Institute, 1993

[5] BERGLUND, B., BERGLUND, U., & Job, R. F. S., Sources and effects of low-frequency noise. Journal of the Acoustical Society of America, 99, 2985e3002, 1996

[6] MOURET, J. & VALLET, M., Les effets du bruit sur la santé. Ministère des affaires sociales de la santé et de la ville, 1995.

[7] European Commission Working Group on Dose-Effect Relations. Position paper on dose response relationships between transportation noise and annoyance. EU's future noise policy, WG2 – dose/effect. Luxembourg: Office for Official Publications of the European Communities; 2002.

[8] MIEDEMA, H. M.; OUDSHOORN, C. G. Annoyance from transportation noise: relationships with exposure metrics DNL and DENL and their confidence intervals. *Environmental health perspectives*, 2001

[9] ANSI S12.9 – Part 4. Quantities and procedures for description

and measurement of environmental sound. Part 4: Noise assessment and prediction of long-term community response. New York: American National Standards Institute, Customer Service Department; 2005.

[10] SCHULTZ, Theodore J. Synthesis of social surveys on noise annoyance. *The journal of the acoustical society of America*, 1978

[11] PIERRETTE, Marjorie, et al. Noise annoyance from industrial and road traffic combined noises: A survey and a total annoyance model comparison. *Journal of environmental psychology*, 2012

[12] MARQUIS-FAVRE, Catherine; PREMAT, Eric; AUBRÉE, D. Noise and its effects–a review on qualitative aspects of sound. Part II: Noise and annoyance. *Acta Acustica united with Acustica*, 2005

[13] NGUYEN, Thu Lan, et al. Structural equation models of road traffic and aircraft noise annoyance in Vietnam. *Noise Control Engineering Journal*, 2018

[14] GILLE, Laure-Anne; MARQUIS-FAVRE, Catherine; LAM, Kin-Che. Structural equation modeling of partial and total annoyances due to urban road traffic and aircraft noises. *The Journal of the Acoustical Society of America*, 2017

[15] BODDEN, Markus. The importance of binaural hearing for noise validation. *Zeitschrift fur Larmbekampfung*, 1994

[16] KIM, Jaehwan, et al. The influence of binaural effects on annoyance for transportation noise. *Noise control engineering journal*, 2007

[17] BERGLUND, Birgitta, et al. Loudness (or annoyance) summation of combined community noises. *The Journal of the*

Acoustical Society of America, 1981

[18] BOTTELDOOREN, Dick; VERKEYN, Andy. Fuzzy models for accumulation of reported community noise annoyance from combined sources. *The Journal of the Acoustical Society of America*, 2002

[19] RONNEBAUM, T.; SCHULTE-FORTKAMP, B.; WEBER, R. Synergetic effects of noise from different sources: a literature study. In: *International congress on noise control engineering*. 1996

[20] SCHULTE-FORTKAMP, B.; WEBER, R. Overall annoyance ratings in a multisource environment. In: *INTER-NOISE and NOISE-CON Congress and Conference Proceedings*. Institute of Noise Control Engineering, 1997

[21] BERGLUND, B.; NILSSON, M. E. Total annoyance and perceptually discernible noise sources. In: *proceedings of InterNoise*. 2000

[22] MIEDEMA, Henk ME. Relationship between exposure to multiple noise sources and noise annoyance. *The Journal of the Acoustical Society of America*, 2004

[23] VOS, Joos. Annoyance caused by simultaneous impulse, road-traffic, and aircraft sounds: A quantitative model. *The Journal of the Acoustical Society of America*, 1992

[24] ZWICKER, Eberhard; FASTL, Hugo. *Psychoacoustics: Facts and models*. Springer Science & Business Media, 2013

[25] MOORE, Brian CJ; GLASBERG, Brian R. A revision of Zwicker's loudness model. *Acta Acustica united with Acustica*, 1996

[26] MOORE, Brian CJ; GLASBERG, Brian R.; BAER, Thomas. A

model for the prediction of thresholds, loudness, and partial loudness. Journal of the Audio Engineering Society, 1997

[27] GLASBERG, Brian R.; MOORE, Brian CJ. A model of loudness applicable to time-varying sounds. Journal of the Audio Engineering Society, 2002

[28] JOHNSON, Marty E., et al. Development of an efficient binaural simulation for the analysis of structural acoustic data. 2003.

[29] MOORE, Brian CJ, et al. A loudness model for time-varying sounds incorporating binaural inhibition. Trends in hearing, 2016

[30] HELLMAN, Rhona P. Growth rate of loudness, annoyance, and noisiness as a function of tone location within the noise spectrum. *The Journal of the Acoustical Society of America*, 1984

[31] HELLMAN, Rhona P. Perceived magnitude of two-tone-noise complexes: Loudness, annoyance, and noisiness. *The Journal of the Acoustical Society of America*, 1985

[32] BERGLUND, Birgitta; PREIS, Anna; RANKIN, Krystyna. Relationship between loudness and annoyance for ten community sounds. *Environment International*, 1990

[33] BOEKER, Eric R., et al. Integrated noise model (INM) version 7.0 technical manual. United States. Federal Aviation Administration. Office of Environment and Energy, 2008.

[34] HEINONEN-GUZEJEV, Marja, et al. Self-report of transportation noise exposure, annoyance and noise sensitivity in relation to noise map information. *Journal of Sound and Vibration*, 2000

[35] BIRK, Matthias, et al. Road traffic noise: self-reported noise annoyance versus GIS modelled road traffic noise

exposure. *Journal of Environmental Monitoring*, 2011

[36] KNAUSS, D., et al. Noise mapping and annoyance. *Noise and Health*, 2002

[37] MIEDEMA, H.M.E, Response function for environmental noise, TNO Report, 1992

[38] MARTIN, M. A., et al. Exposure–effect relationships between road traffic noise annoyance and noise cost valuations in Valladolid, Spain. *Applied acoustics*, 2006

[39] LIM, Changwoo, et al. Effect of background noise levels on community annoyance from aircraft noise. *The Journal of the Acoustical Society of America*, 2008

국문초록

항공기와 도로 교통 소음의 복합 소음에 대한 불쾌감 평가 모델 개발 및 인지적 소음지도 작성

전찬일

서울대학교 대학원

기계항공공학부

교통 시스템의 발달로 인해 항공기와 도로 교통 소음의 복합 소음에 대한 노출이 증가하고 있다. 이러한 복합 소음에 대한 반응은 단일 소음원의 경우와 다르기 때문에 기존의 방법과 다르게 평가해야 한다. 기존의 평가 방법은 소음의 물리적 수준만을 가지고 평가하고 있지만 불쾌감 지표는 심리음향학 지표이기 때문에 같은 인지적 지표를 통해 평가해야 한다. 다른 연구 결과에 따르면 불쾌감과 가장 밀접한 관련이 있는 지표는 라우드니스 지표로서 본 연구에서는 라우드니스 지표를 통해 불쾌감을 평가하였다.

복합 소음의 라우드니스를 계산하기 위해 양쪽 귀의 영향을 고려한 새로운 파셜 라우드니스 모델을 개발하고 이를 검증하였다. 새로운 모델을 통해 단기 및 장기 노출에 대한 불쾌감 평가 모델을 제시하였다.

항공기와 도로 교통 소음의 복합 소음에 대한 단기 불쾌감 평가 모델은 실험실 내 환경에서 실험을 통해 도출하였고 로지스틱 회귀분석을 통해 라우드니스와 불쾌감 사이의 관계식을 도출하였다.

복합 소음에 대한 장기 불쾌감 평가 모델은 설문조사와 소음지도 작성을 통해 개발하였다. 소음지도를 통해 항공기와 도로 교통 소음의 소음도를 추출하여 파셜 라우드니스를 계산하였고 이를 설문조사 결과와의 로지스틱 회귀분석을 통해 관계식을 도출하고 이를 소음 지도 작성 프로그램에 적용하여 인지적 소음지도를 작성하였다. 인지적 소음지도를 통해 소음 노출 지역에 대한 불쾌감을 한눈에 파악하고 또한 배경 소음에 대한 영향을 확인할 수 있다.

주제어: 복합 소음, 파셜 라우드니스, 불쾌감 평가 모델, 인지적 소음지도

학번: 2013-20711